Some Mineralogical Characteristics of the Egyptian Black Sand Beach Ilmenite Part I: Homogeneous Ilmenite and Titanhematite-Ferriilmenite Grains

Mohamed Ismail Moustafa
Northern Border University, Saudi Arabia and
Nuclear Materials Authority, Cairo, Egypt
ismail2251962@yahoo.com

Received: 30 August 2022 | Revised: 15 September 2022 | Accepted: 17 September 2022

Abstract-The high-grade Egyptian beach ilmenite concentrate contains various mineral textures in addition to the main homogeneous ilmenite grains (63%), which may contain solid solutions of geikielite ($MgTiO_3$) and pyrophanite ($MnTiO_3$) mineral components. Few homogeneous ferriilmenite grains (2%) associated with the concentrated ilmenite grains are detected. The contents of Fe_2O_3, MgO, Al_2O_3, and Cr_2O_3 in the ferriilmenite grains range between 7.3% and 22.8%, 3.4% and 6.6%, 0.2% and 0.7%, and 0% and 1.2% respectively. The detected hematite-ilmenite exsolved intergrowths (21.4%) have titanhematite exsolutions of different shapes, sizes, and orientations. They occupy 5%-40% of the whole intergrowth and may show one or two distinct generations. In some ferriilmenite components, MnO ranges between 1.5% and 8.6%. The Cr_2O_3 and Al_2O_3 contents range between 0% and 1.2% and 0% and 3.2% respectively. They are mostly between 0% and 0.1% for either of the ferriilmenite components, while relatively greater content is present in the titanhematite components. In some grains, the titanhematite exsolution bodies are replaced by goethite or hydrated iron oxides. In others, the ferriilmenite intergrowth may be partially or completely altered into leucoxene. Some minor composite grains are detected in the concentrate, where each grain consists of two parts, one part is titanhematite-ferrimenite and the other is ferriilmenite-titanhematite. The titanhematite exsolved components have relatively lower TiO_2 content (5.8%-23.8%). Both MgO and MnO are positively correlated with FeO rather than Fe_2O_3. The presence of sphene in the obtained ilmenite concentrate may be responsible for the recorded amounts of SiO_2 and CaO. The Cr_2O_3 content is relatively much higher in sphene spots than in ilmenite spots, ensuring that Cr_2O_3 neither follows TiO_2 nor FeO. The nature of the problem of the relatively lower Ti content and the relatively higher Fe and Cr contents of the obtained ilmenite concentrates is the target of the article. The problem is related to the mineralogy of ilmenite or to the used physical concentration flowsheet of the separated concentrate and the ability to improve the ilmenite concentrate's specifications. It is concluded that although the homogeneous ilmenite is characterized by low Cr_2O_3 content, some of the other exsolved texture components, e.g. titanhematite and sphene, have relatively higher Cr_2O_3, in addition to Fe_2O_3, SiO_2, or CaO. They can negatively affect the marketable specifications of the separated Egyptian black sand ilmenite concentrate.

Keywords-beach ilmenite; geikielite; pyrophanite; ferriilmenite; titanhematite; Egypt

I. INTRODUCTION

The Egyptian black sand contains huge reserves of 6 common economic minerals, i.e. ilmenite, magnetite, garnet, zircon, rutile, and monazite in descending order of abundance. The Egyptian black sand is present either as beach sands (Figure 1, (1)), or coastal sand dunes. The Egyptian black sand minerals are derived originally from the disintegration of rocks, they are carried by the Nile waters, and are deposited after the river meets the Mediterranean Sea. The Egyptian black sand is considered in general as Recent to Pleistocene in age [1]. The deposit mainly contains the 6 above mentioned minerals. They are associated with quartz and green silicates (amphiboles and pyroxenes). Traces of cassiterite, gold, and Pb, Zn, Hg, Ag, Th, U, Nb, Ta, and Pt minerals have also been detected [2-4]. Along the north coast of Egypt, in areas characterized by extensive beach erosion, east and west of the Rosetta estuary, some surfacially highly concentrated black sands are found parallel to the shoreline. They form narrow patches with lengths that rarely attain 1Km and widths ranging from a few up to 60m [2]. However, the original amount of materials transported by the river may be related to several variables such as the flow type and the sediment load [5].

Ilmenite ($FeTiO_3$) is the most abundant titanium mineral. The main source of ilmenite, rutile and leucoxene, are the sand type placer deposits found at or near the coast. Ilmenite also occurs in massive rock formations in the form of titaniferous iron ores, associated with hematite and magnetite [6]. Ilmenite and rutile are used for the manufacture of titanium dioxide white pigment which is the whitest and most stable of all known white pigments, being entirely unaffected by acids or alkalies that dissolve and destroy other whites. It has the good ability to maintain its visual appearance for a considerable period of time. It is stable up to 1800°C. Ilmenite is also used for the production of metallic titanium which is characterized by high strength in relation to its density, the ability to retain its properties from -300°F to 1000°F, and its excellent corrosion resistance. Titanium forms extremely hard metallic compounds

Corresponding author: Mohamed Ismail Moustafa

with carbon, silicon, nitrogen, and boron. They are used as tips for cutting tools and in abrasive stones and wheels [6-7].

The majority of the mineralogical features of the Egyptian beach ilmenite can be seen in [2, 8-16]. Many authors have reported the relatively lower TiO_2 content and the relatively higher Fe_2O_3 and Cr_2O_3 contents, while others reported the diversity of the mineralogical textures inside ilmenite grains. However, the ilmenit content of the Egyptian black sand ranges from less than 1% in the raw beach sand up to more than 50% in the naturally highly concentrated surfacial black sands. Most of the obtained Egyptian beach ilmenite concentrates are characterized by a relatively lower TiO_2 content (44-46% of ilmenite's beach sand and 46-49 wt% of ilmenite's sand dunes) and relatively greater Cr_2O_3 content (0.1-0.4%). Also, they have a relatively lower Fe^{2+}/Fe^{3+} ratio and relatively higher MgO and MnO contents.

The ilmenite ore of Abu Ghalaga mine, south eastern Desert of Egypt, occurs as massive-type interlayer gabbroic rocks [17]. The massive ilmenite ores are considered the second major type of Fe-Ti oxide mineral ores in Egypt. Authors in [18] explained that Abu Ghalaga ilmenite ore is not found as homogeneous grains but it is mainly hematite-ilmenite exsolution texture containing 36.78% TiO_2, 25.85% FeO, 29.86% Fe_2O_3, and 4.46% SiO_2 along with other minor oxides of Mg, Mn, Cr, and P. Abu Ghalaqa and Korabkanci, south eastern Desert of Egypt, are considered two promising areas of Fe–Ti massive ore deposits [19]. The separation of ilmenite and other economic mineral concentrates from the Egyptian beach sand and other deposits are explained in [2-3, 20]. The majority of ilmenite mineral varieties are contained in the obtained highly purified concentrates using wet gravity concentration and magnetic and high tension electrostatic separation techniques. These varieties are characterized by strongly to moderate magnetic susceptibilities. Except of magnetite, some minor ilmenite varieties associated with hematite, chromite, and definite magnetic leucoxene varieties are separated in definite magnetic fractions characterized by magnetic susceptibilities ranging from the ferromagnetic to the weakly paramagnetic [2].

The problem of relatively higher Cr_2O_3 and Fe_2O_3 contents in the Egyptian beach ilmenite concentrate is the subject of this article. The mineralogical characters of some different ilmenite grains will be investigated. It is necessary to detect if the problem of the high chromium and ferric iron contents in the obtained beach ilmenite concentrates is related to the used ore dressing techniques, or related to the mineralogical features of the obtained ilmenite concentrate. Answering this question can lead to the improvement of the chemical specifications and the economic marketability of the Egyptian beach ilmenite. Lowering the chromium content of the obtained concentrate can improve its use in the white pigment industry.

II. MATERIALS AND METHODS

A bulk sample weighing about 1000 tons was collected from the surfacial naturally highly concentrated beach black sands (Figure 1, (2)), at the Mediterranean coast, 7km east of Rosetta estuary (Figure 1, (1)). The sample represents the raw sand in a 2km stretch with varying width of a few up to 20m. The sands were manually scraped from the mantle to a depth ranging between 10 and 30cm. Using the difference in physical characters between the various economic minerals, the collected surfacial naturally highly concentrated beach raw sands were processed in the plant at Abu Khashaba site (Figure 1, (3)), using the following equipment: Full- and half- size Wilfley shaking tables for wet-gravity concentration, Carpco (HP 167) high-tension roll-type electrostatic separator for electrostatic separation, Reading cross–belts magnetic separator, and the Carpco (MIH 13-231-100) industrial high intensity induced roll dry magnetic separator for magnetic separation. Finally, a bulk conductor ilmenite fraction was obtained and subjected to the refining magnetic stage using the reading cross-belt magnetic separator, where an ilmenite concentrate assaying 99.5% ilmenite grains was obtained.

Four polished sections were prepared from 4 small representative samples and were studied under the reflected microscope and Cameca SX-100 microprobe instrument. They were taken from the obtained final ilmenite concentrate (including 2 obtained magnetic fractions of the separator), a representative sample of the obtained ferromagnetic fraction, a representative sample of all the other obtained magnetic fractions of the separator, and, finally, a representative sample of the obtained non magnetic fraction of the separator.

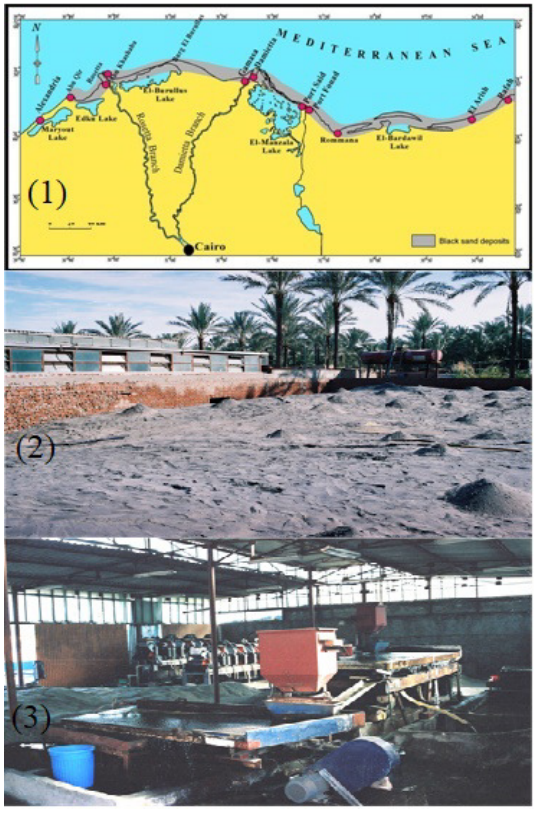

Fig. 1. (1) Distribution of the Egyptian black sand showing the location of the surfacial naturally highly concentrated beach black sand 7 km to the east of Rosetta estuary, Abu Khashaba. (2) The collected bulk sample of the surfacial beach black sand, dried by sunlight. (3) A part of the physical concentration plant at Abu Khashaba showing the full- and half-size Wilfley shaking tables and the two R cross belt magnetic separators.

The investigation of the different ilmenite grains was carried out by a Cameca SX-100 Electron Microprobe Analyzer (EMPA), from the Institute of Mineralogy and Crystal Chemistry, Stuttgart University, Germany. The microprobe instrument is equipped with 3 Wavelength Dispersive Spectrometers (WDS) and an Energy Dispersive Spectrometer (EDS). The whole surface of the polished sections was examined by Back Scattered Electron (BSE) images, so that ilmenite grains with 10μm size or even smaller could be detected. The analytical conditions were 15kV accelerating voltage, 15nA electron current, 180s counting time for each analyzed spot, and 1 to 4μm diameter of the focused electron beam. The following standards were used: diopside for Mg and Ca, albite for Na, corundum for Al, orthoclase for Si and K, rutile for Ti, rhodonite for Mn, Fe_2O_3 for Fe, Cr_2O_3 for Cr, V for V, and sphalerite for Zn. Kα lines were used for the element analysis. Also, a binocular microscope, a reflected-light polarizing microscope, sample splitters, and various containers were utilized.

III. CALCULATION

A. Calculation of the Fe^{3+} Content and the Molecular Formula of the Studied Ilmenite Grains

In the current paper, using the formula of [21], a constructed ilmenite formula in Microsoft Excel was used for the calculation of the Fe^{3+} content and the molecular formula of of ilmenite mineral component of the studied individual ilmenite grains.

B. Calculation of Different Mineral Components of the Analyzed Spots Composed Mainly of Ferriilmenite and/or Titanhematite with or without Individual TiO_2 (Rutile)

Most of the analyzed spots of the grains were subjected to one of the following calculation methods to determine the different mineral fraction components of each analyzed spot.

1) The First Method (M1)

In this method, the adopted ilmenite Excel formula was carried out for each analyzed spot to calculate FeO % and Fe_2O_3 %. If the sum of cations is less than 2, then all iron content must be considered as FeO, completely contained within the calculated ilmenite fraction component. The calculated iron fraction as FeO % (cal) is used to calculate the corresponding content of ilmenite fraction ($FeTiO_3$), and its corresponding content of TiO_2 wt% as follows: ilmenite mineral fraction = FeO % (cal) × 2.112, included TiO_2 % = FeO % (cal) × 1.112 or = ilmenite mineral fraction (cal)/1.9. These values are concluded from (1):

$$FeO + TiO_2 = FeTiO_3 \text{ (ilmenite)} \quad (1)$$

Then:

$$71.85 \text{ g FeO} + 79.87 \text{ g } TiO_2 = 151.72 \text{ g } FeTiO_3$$

Or:

$$47.36 \text{ \% FeO} + 52.64 \text{ \% } TiO_2 = 100 \text{ \% ilmenite}$$

In ilmenite we have: TiO_2/FeO = 1.112, ilmenite/FeO = 2.112, and ilmenite/TiO_2 = 1.9. The calculated Fe_2O_3 % of the analyzed spot will be considered as hematite mineral component %. The MgO % and MnO % contents of the analyzed spot are used for the calculation of the corresponding contents of individual geikielite ($MgTiO_3$) and pyrophanite ($MnTiO_3$) mineral components and also their corresponding individual contained TiO_2 %. The calculation of these values depends on the following equations:

$$MgO + TiO_2 = MgTiO_3 \text{ (geikielite)} \quad (2)$$

Then:

$$40.31 \text{ g MgO} + 79.87 \text{ g } TiO_2 = 120.18 \text{ g geikielite}$$

Or:

$$33.54 \text{ \% MgO} + 66.46 \text{ \% } TiO_2 = 100 \text{ \% geikielite}$$

$$MnO + TiO_2 = MnTiO_3 \text{ (pyrophanite)} \quad (3)$$

Then:

$$70.94 \text{ g MnO} + 79.87 \text{ g } TiO_2 = 150.81 \text{ g pyrophanite}$$

Or:

$$47.04 \text{ \% MnO} + 52.96 \text{ \% } TiO_2 = 100 \text{ \% pyrophanite}$$

Hence, in geikielite, TiO_2/MgO = 1.982, geikielite/MgO = 2.982, and geikielite/TiO_2 = 1.51. In pyrophanite, TiO_2/MnO = 1.126, pyrophanite/MnO = 2.126, and pyrophanite/TiO_2 = 1.89.

The remaining individual TiO_2 % (rutile) component can be calculated by subtracting the sum percentages of TiO_2 contained in the calculated ilmenite, geikielite, and pyrophanite individual mineral components from the bulk analyzed TiO_2 % of the analyzed spot. All the calculated contents of the mineral fractions inside the analyzed spot are added to obtain the total sums. If the calculated individual TiO_2 % has a negative value, the contained TiO_2 in the calculated three mineral fractions is higher than the actual bulk analyzed TiO_2 % of the spot. There are four reasons for this: At first, there are other analyzed oxides that must be considered and added with the analyzed TiO_2 % of the spot to be included within the bulk TiO_2 content of the spot. Also, there are some values of the analyzed oxides FeO, MgO, MnO, not included in their corresponding calculated mineral components. The third reason is that some analyzed oxides are impurities such as SiO_2 CaO, which cannot be neglected and the other analyzed oxides must be corrected. The fourth reason is that it is obvious that the content of individual TiO_2 content of the analyzed spot is negligible. However, if the obtained individual TiO_2 % values are equal to – 0.01 down to – 0.05 or even –0.1, these values may be due to the rounding to two decimal places for most of the treated oxides. These negative values can be neglected and the content of individual TiO_2 is considered as zero. However, in the case of obtained negative values, the second method of calculation is recommended.

2) The Second Method (M2)

In this method (M2), we act directly to the analyzed oxides of the detected spot, and the adopted ilmenite Excel formula is not applied. The contents of ilmenite mineral fractions are calculated directly from the analyzed TiO_2 % and not from the calculated FeO %. This method of calculation includes the following steps:

The calculation of the geikielite mineral content from the analyzed MgO % of the spot, the calculation of pyrophanite mineral content from the analyzed MnO % of the spot, and the calculation of the remaining TiO_2 % (R TiO_2) is conducted as follows:

$$R\ TiO_2 = \text{the analyzed } TiO_2 \text{ of the spot - [}TiO_2 \text{ contained in geikielite + } TiO_2 \text{ contained in pyrophanite]} \quad (4)$$

Then, R TiO_2 = TiO_2 of the spot – [MgO % × 1.982 + MnO % × 1.126]. If the result of the last equation equals to zero or a negligible negative value, then there is no ilmenite in the analyzed spot.

In the case of the presence of excess TiO_2, then:

$$\text{Ilmenite mineral fraction} = R\ TiO_2 \times 1.9 \quad (5)$$

The FeO % contained in the calculated ilmenite is calculated as follows:

$$\text{FeO \% contained in ilmenite} = \text{calculated ilmenite \%} / 2.112 \quad (6)$$

$$R\ FeO \text{ of the analyzed spot} = \text{the analyzed FeO \% of the spot} - \text{the calculated ilmenite \%} / 2.112 \quad (7)$$

If the analyzed TiO_2 % of the spot is completely entering in the calculated ilmenite fraction, and there is no hematite fraction in the analyzed spot, then the contained FeO % of the calculated ilmenite fraction will be exactly equal to the analyzed one.

If the result of (7) has a positive value, then there is a content of Fe_2O_3 fraction in the analyzed spot, equal to R FeO × 1.1113. Both the analyzed contents of Cr_2O_3 and Al_2O_3 of the spot are added with the calculated Fe_2O_3 % and are considered to represent the present hematite fraction of the analyzed spot. The V_2O_3 content is not added to the content of the hematite because it was noticed that V_2O_3 may follow Fe_2O_3 and sometimes TiO_2. Finally, the sum for all the determined mineral fractions was calculated.

3) The Third Method (M3)

This method of calculation is used with analyzed spots composed mainly of ferriforous rutile. It is a modified form of M2, where all the analyzed FeO % is completely considered as representative of the hematite mineral fraction. Both analyzed MgO % and MnO % are used to calculate the corresponding individual mineral fractions of geikielite and pyrophanite respectively. The remaining TiO_2 % after subtracting the TiO_2 contents included within both geikielite and pyrophanite mineral fractions from the bulk analyzed sample of the spot is considered to represent the individual TiO_2 phase in the analyzed spot. In summary, the first method (M1) of calculation is used when there is a definite amount of individual TiO_2 and the adopted ilmenite program must be used in this method to determine the contents of FeO and Fe_2O_3. M2 is used when there is no an individual content of TiO_2 while M3 is used when there is no ilmenite mineral fraction. In the two last methods, the application of the adopted ilmenite program is not required and we act directly with the the original analyses of detected oxides.

IV. RESULTS

A. General

The investigation of the different mineral textures in the obtained ilmenite concentrate and the other obtained magnetic fractions reflects that, except magnetite, the naturally highly concentrated surfacial black sands contain 42.65% different ilmenite mineral varieties and 2.51% other opaques, mainly hematite and chromite, in a total of 45.16%. It also contains 1.85% of completely altered ilmenite varieties, 1.48% magnetic and 0.37% non magnetic highly leucoxenated grains [2]. Various mineral textures were detected under the microscope. Their content percentages and their chemical compositions were calculated and investigated. 48 analyzed spots within 7 grains of homogeneous ilmenite that have Mg content relatively higher than Mn have been investigated. 26 analyzed spots within 5 homogeneous ferriilmenite grains with relatively higher Mg than Mn content were detected. Another 51 analyzed spots contained within 6 grains of homogeneous ilmenite have relatively higher Mn content. 82 other analyzed spots within 7 grains of titanhematite-ferriilmenite exsolved intergrowth and 2 composite grains consisting of 2 parts of titanhematite-ferriilmenite and ferriilmenite-titanhematite exsolved intergrowths. The corresponding different mineral component fractions of the inhomogeneous spots of the last 82 analyzed spots were also calculated. Finally, 17 analyzed spots within 3 grains of partially altered ilmenite into sphene were also investigated. The analyzed oxides of the detected spots include TiO_2, FeO, Fe_2O_3, Cr_2O_3, MnO, MgO, Al_2O_3, V_2O_3, ZnO, SiO_2, and CaO. The ilmenite molecular formula of homogeneous ilmenite spots and various mineral component fractions of the inhomogeneous analyzed spots were calculated.

B. Microscopic Investigation

The homogeneous ilmenite includes grains that appear completely homogeneous under the reflected light microscope. The majority of the grains are elongated to globular, with tabular and rod-shaped not being uncommon (Figures 2-3). Their color is dull grey with distinct brownish tint. Some grains have a characteristic reddish or pinkish brown tint. Others have relatively darker brown colors. The majority of ilmenite grains have strong pleochroism from light to a relatively darker brown color. Under crossed nicols, the homogenous ilmenite grains have strong anisotropism and change from bright, relatively lighter, brown to dull, relatively darker, brown colors. Inner reflections are generally absent. Lamellar twining is sometimes observed where twin lamellae exist in one direction along the rhombohedral 1011 planes. The relative darkness or lightness of brown colors for some of ilmenite grains may be related to the presence of either geikielite ($MgTiO_3$) or pyrophanite ($MnTiO_3$) in solid solutions with ilmenite. The ilmenite grains which probably contain geikielite solid solution, show darker color, lower reflectivity, and a reddish brown internal reflection, when compared to normal ilmenite [9]. On the other hand, pyrophanite resembles ilmenite, but shows lower reflectivity, less brown color, less strong bireflectance, anisotropism, and often beautiful reddish internal reflections [22]. Some rare ilmenite grains were found to be composed of several aggregates in the form of more or less idiomorphic grains, with intergranular films of transparent spinel granules.

When rotating the stage of the microscope, the aggregates show irregular boundaries and different positions in relation to their reflection pleochroism. However, the aggregates and their boundaries are more pronounced under the crossed nicols due to the different positions of their distinct anisotropy. This feature may be the result of deformation and recrystallization of the ilmenite during metamorphism accompanied by the migration of spinel to the grain borders [23]. Homogeneous ferriilmenite grains (Figure 2 (8)-(12)), were detected to have paler colors and relatively higher reflectivities with very light brownish tints than the normal ilmenite. The grains are ferromagnetic or strongly paramagnetic with relatively stronger mass-magnetic susceptibilities than the majority of homogenous ilmenite or titanhematite-ferriilmenite exsolved grains. Most of the grains are even lighter than titanomagnetite grains. The majority of homogeneous ferriilmenite grains have weak reflection pleochroism while under crossed nicols they have strong and distinct anisotropism. These ferriilmenite grains are the result of a considerable amount of Fe_2O_3 in the solid solution. Some of the ferromagnetic and strongly paramagnetic ferriilmenite grains were found to contain exsolution bodies of titanhematite with their long axes parallel to each other and to the (0001) direction of ilmenite. However, such exsolutions do not exceed 10 to 15% of the whole intergrowth and are particularly found as fine seriate exsolution lamellae.

The hematite-ilmenite exsolution intergrowth texture is called hemoilmenite where microintergrowths of titanhematite or ilmenohematite are enclosed in the ferrian ilmenite [24]. In a considerable number of the titanhematite-ferriilmenite exsolved intergrown grains, most of the oriented titanhematite exsolution bodies are replaced by goethite or limonite while the host ferriilmenite remains unchanged (Figure 4 (1)). Some of the replaced titanhematite exsolution bodies give grey material with distinct anisotropism and obvious bluish tint relatively much lighter under the reflected light. Sometimes brownish yellow internal reflection colors are observed. This material is certainly goethite. Sometimes, some positions in the exsolved titanhematite lamellae seem to be altered to fine grained goethite or to fine aggregates of hydrated iron oxides which are dark in color, nearly isotropic and showing yellow to yellowish brown internal reflections. In this intergrowth, the titanhematite exsolutions show different shapes, sizes, and orientations in the different titanhematite-ferriilmenite grains. In most of them, the exsolution bodies of titanhematite occur in ferriilmenite with their long axes parallel to each other and to the (0001) direction of the ilmenite, showing only one generation of exsolved titanhematite (Figure 4, (2)-(4)). Some show 2 distinct generations of exsolutions. The exsolution bodies of the first generation, relatively coarser, contain fine seriate exsolutions of ferriilmenite parallel to the (0001) direction of titanhematite. The second generation, on the other hand, is relatively finer and generally parallel to the first titanhematite generation bodies and to the (0001) direction of the ferriilmenite. The titanhematite may be also found as banded or rectilinear exsolution intergrowths traversing the whole ilmenite grain. Other grains contain lensoid to elongated broad blades of exsolved intergrowths of titanhematite alternating with broad plates of the host ferriilmenite. In these two last cases, both titanhematite and ferriilmenite exhibit swarms of oriented fine seriate exsolution bodies (Figure 4, (5)-(6)).

V. Discussion

A. Homogeneous Ilmenite (63%) and Homogeneous Ferriilmenite (2%)

The homogeneous ilmenite represents the major component of the obtained ilmenite concentrate. It was found out that the investigated homogeneous grains contain both Mg and Mn in their chemical composition. Some of these grains have more Mg content than Mn, some the opposite.

1) Homogeneous Ilmenite and Ferriilmenite with more Mg than Mn content

According to [25-26], Mg-ilmenites (picroilmenites) indicate derivation of magmas from subcontinental mantle lithosphere. Authors in [27] explained that higher Mg concentrations are typically associated with more primary ilmenite grains almost 45-55 wt% TiO_2, while authors in [28] explained that Mg-rich ilmenite is typical of mafic igneous rocks. However, the Nile river drainage has various rock types and hence, various types of ilmenite grains. Some of the investigated homogeneous ilmenite grains contain much more MgO than MnO. The 12 grains of Figure 2 (Table I), are examples of these grains. Grains (1)-(7) are detected in the obtained final ilmenite concentrate. In spot 1 (Figure 2(1), Table I), an inclusion of SiO_2 (18.82%) is associated with ilmenite. Neglecting the SiO_2 content and the recalculation of the analyzed spots by multiplying by [100/(100-18.82)], spot 1 gives a well-defined ilmenite chemical formula (Table I). The other analyzed spots are ilmenite with a slight content of dissolved Fe_2O_3. Spots 1-12 of grain (2) are ilmenite with definite dissolved Fe_2O_3. The iron content of spots 13 and 14 is totally ferrous, the sums of cations are 2 and 1.97 respectively. In comparing these 2 spots with the other analyzed spots of the grain, it is obvious that most of their ferric iron content is leached out and some molecular water is included within their pores. The sums of total oxides are 95.4% and 92.6% respectively. These 2 spots contain also considerable amounts of molecular water. Grains (3)-(4) are ilmenite with some mixed Fe_2O_3 content as solid solutions. In the grains (1)-(4), the contents of mixed Fe_2O_3 ranges are 4.73-- 7.60%, 3.88-5.66%, 4.28-6.03%, and 3.85-4.32% respectively. In grain (5), spots 1 and 7 are beside or inside a crack of the grain. Hence, their lower sum of total oxides. In this grain, the Fe_2O_3 content ranges between 2.58 (spot 7) and 7.58 (spot 1). Both spots may contain considerable amounts of molecular water. Grains (6)-(7) are ilmenite with some mixed Fe_2O_3 content ranging between 3.71 and 6.01%. Spot 8 of grain (6) is found to be leached ilmenite. A constructed Excel forumla was used for the identification and calculation of the leached ilmenite.

2) Homogeneous Ferriilmenite

Ferriilmenite grains (8)-(12) of Figure 2 (Table I) were detected within the ferromagnetic fraction associated with magnetite and titanomagnetite grains and contain relatively higher contents of mixed Fe_2O_3, which are 22.47-22.81%, 7.33-8.72%, 21.01-22.05%, 14.52-15.25%, and 9.4-14.64% respectively.

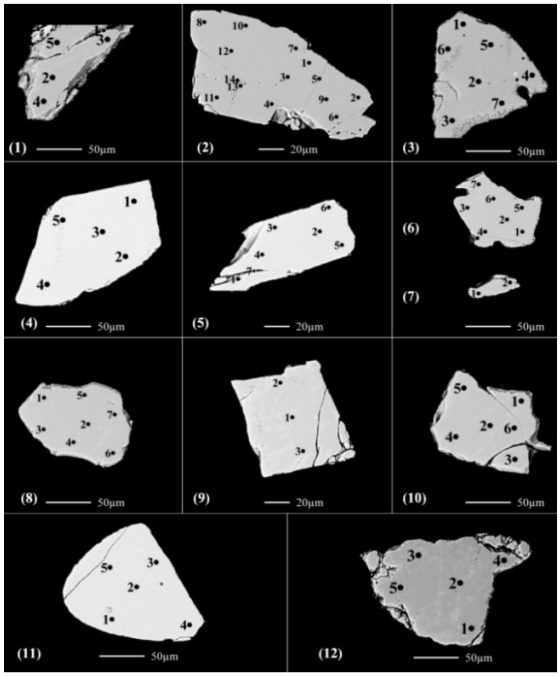

Fig. 2. BSE images of the homogeneous ilmenite grains: (1)-(7), have more Mg than Mn content. (8)-(12) are homogeneous ferriilmenite grains.

However, MgO and Al_2O_3 contents are also relatively higher in these grains, ranging between 3.38-3.57 % and 0.2-0.25% in grain (8), 3.81-4.05% and 0.21-0.28% in grain (9), 4.38-4.65% and 0.35-0.40% in grain (10), 5.41-5.56% and 0.39-0.46% in grain (11), and 4.57-6.6% and 0.23-0.65% in grain (12) respectively. Also, the Cr_2O_3 content in these grains is relatively higher, especially in grain (11). It ranges between 1.04 and 1.21% in grain (11), while it ranges between 0 and 0.31% in the other 4 grains. Comparing these grains with the last 7 grains ensures that Al_2O_3 follows Fe_2O_3. The content of Al_2O_3 increases as the contents of Fe_2O_3 increases.

3) Homogeneous Ilmenite with More Mn than Mg Content

Mn-rich ilmenite tends to be abundant in peraluminous granite and metapelite, and is thus characteristic of ilmenite with abundant unoriented quartz inclusions [28]. The values for MnO in ilmenite from Jacupiranga Cabonatite, Brazil, range between 2.2 and 3.5% with one sample having 7.9% [29-30]. The MnO content of ilmenite from Chhatrapur coast, Odisha, India, varies from 0.125 to 0.579% while the MgO content varies from 0.069 to 1.357%, indicating a solid solution series between ilmenite, pyrophanite, and geikielite [31]. In coexisting magnetite and ilmenite, MgO and MnO partition preferentially into ilmenite. MgO shows a regular pattern of distribution between them, whereas MnO is distributed irregularly [32].

Another type of ilmenite grains in the final obtained ilmenite concentrate is detected where the Mn content is larger than the MgO. These grains are shown in Figure 3, Table II as follows: in grain (1), most of the analyzed iron content is ferrous iron. Spot 1 is in a crack while spot 10 is leached ilmenite. Grain (2) is ilmenite with minor Fe_2O_3 content in spots 1-3. The iron content of spots 3-5 is mainly ferrous iron. In grain (3), the analyzed iron content of all the analyzed spots is ferrous iron. In grain (4), ilmenite is mixed with 3.03-4.96% Fe_2O_3 content. In grains (5) and (6), the content of MnO is relatively higher and ranges between 2.67 and 3.46% for (5) and 4.52 and 6.09% for (6). Their Cr_2O_3 content is negligible. The content of mixed Fe_2O_3 in these 2 grains is relatively higher, ranging between 14.9 and 18.01% in (5) and 3.41 and 10.22% in (6). The content of Al_2O_3 is not positively correlated with the content of Fe_2O_3 in the analyzed spots. Also, in grain (6), the comparison of spots 1, 3, 5, and 9 with the others reveals that ilmenite is altered in these 4 spots into individual phases of TiO_2 and Fe_2O_3 where some of the Fe_2O_3 content is leached out. In spot 1, some of the SiO_2 content is mixed where a relatively lower content of TiO_2 wt% is recorded. Due to the presence of these 4 spots on the edge of the grain, the process of alteration is relatively higher. Hence, there are appreciable contents of molecular water inside them (Table II).

B. Hematite-Ilmenite Exsolution Intergrowth (21.4%)

The most common exsolved intergrowth type in the examined ilmenite grains is the titanhematite-ferriilmenite exsolved intergrowths. The same was also reported in [8, 33]. Similar textures of titanhematite exsolution bodies were found in [34], showing that in the majority of grains, the hematite occupies about 20 to 25% of the intergrowth. It was also shown that very coarse intergrowths are occassionally observed where the hematite occupies about 30-35% of the whole intergrowth. On the other hand, the percentage of the titanhematite intergrowths in ilmenite does not exceed 5% in some mineral deposits of Um Rus Area, Eastern Desert, Egypt [35].

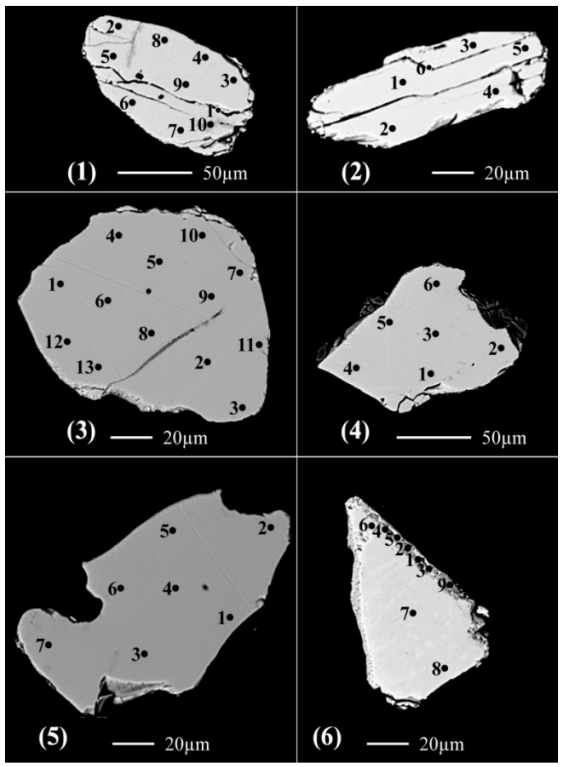

Fig. 3. BSE images of homogeneous ilmenite grains with more Mn than Mg content.

TABLE I. MICROPROBE CHEMICAL ANALYSIS AND CORRESPONDING MOLECULAR FORMULAE OF THE ANALYZED SPOTS FOR HOMOGENEOUS ILMENITE GRAINS WITH A RELATIVELY HIGHER Mg CONTENT, GRAINS (1)-(7) AND FERRIILMENITE GRAINS (8)-(12) OF FIGURE 2

Grains	Spots	SiO_2	MgO	MnO	CaO	ZnO	FeO	Al_2O_3	V_2O_3	Cr_2O_3	TiO_2	Total	SiO_2	MgO	MnO	CaO	ZnO	FeO	Fe_2O_3	Al_2O_3	V_2O_3	Cr_2O_3	TiO_2	Total	Fe ferrous	Fe ferric	Other cations	Ti	O
	1	18.82	0.70	0.46	0.26	0.05	39.61	0.06	0.36	0.08	40.17	100.56	18.82	0.70	0.46	0.26	0.05	56.56	18.84	0.06	0.36	0.08	40.17	98.68	1.12	-0.34	0.47	0.72	3
	1	0.00	0.86	0.57	0.32	0.06	48.72	0.07	0.44	0.10	49.41	100.55	0.00	0.86	0.57	0.32	0.06	41.88	7.60	0.07	0.44	0.10	49.41	101.31	0.87	0.14	0.07	0.92	3
Fig. 2	2	0.00	1.19	0.60	0.00	0.03	47.67	0.03	0.42	0.01	50.33	100.29	0.00	1.19	0.60	0.00	0.03	42.52	5.73	0.03	0.42	0.01	50.33	100.86	0.88	0.11	0.07	0.94	3
(1)	3	0.00	1.19	0.67	0.01	0.00	48.00	0.01	0.42	0.00	50.60	100.90	0.00	1.19	0.67	0.01	0.00	42.71	5.89	0.01	0.42	0.00	50.60	101.49	0.88	0.11	0.07	0.94	3
	4	0.00	1.16	0.57	0.01	0.00	48.15	0.00	0.45	0.00	50.82	101.17	0.00	1.16	0.57	0.01	0.00	43.06	5.66	0.00	0.45	0.00	50.82	101.73	0.89	0.11	0.06	0.94	3
	5	0.00	1.26	0.59	0.02	0.00	47.18	0.02	0.45	0.00	50.90	100.42	0.00	1.26	0.59	0.02	0.00	42.92	4.73	0.02	0.45	0.00	50.90	100.89	0.89	0.09	0.07	0.95	3
	1	0.00	1.12	0.52	0.03	0.14	46.13	0.00	0.45	0.01	48.61	97.02	0.00	1.12	0.52	0.03	0.14	41.03	5.66	0.00	0.45	0.01	48.61	97.58	0.88	0.11	0.07	0.94	3
	2	0.00	1.13	0.42	0.01	0.02	46.30	0.00	0.48	0.02	48.58	96.96	0.00	1.13	0.42	0.01	0.02	41.23	5.63	0.00	0.48	0.02	48.58	97.52	0.89	0.11	0.06	0.94	3
	3	0.00	1.18	0.43	0.00	0.00	45.74	0.01	0.40	0.00	48.97	96.73	0.00	1.18	0.43	0.00	0.00	41.52	4.69	0.01	0.40	0.00	48.97	97.20	0.90	0.09	0.06	0.95	3
	4	0.00	1.17	0.48	0.01	0.07	46.00	0.00	0.45	0.04	48.97	97.20	0.00	1.17	0.48	0.01	0.07	41.40	5.11	0.00	0.45	0.04	48.97	97.70	0.89	0.10	0.07	0.95	3
	5	0.00	1.13	0.47	0.04	0.04	45.55	0.00	0.46	0.03	49.00	96.72	0.00	1.13	0.47	0.04	0.04	41.51	4.49	0.00	0.46	0.03	49.00	97.17	0.90	0.09	0.07	0.95	3
	6	0.02	1.11	0.50	0.00	0.06	45.91	0.02	0.40	0.02	49.02	97.06	0.02	1.11	0.50	0.00	0.06	41.58	4.81	0.02	0.40	0.02	49.02	97.54	0.89	0.09	0.07	0.95	3
Fig. 2	7	0.00	1.16	0.40	0.00	0.00	45.41	0.00	0.40	0.04	49.09	96.49	0.00	1.16	0.40	0.00	0.00	41.69	4.13	0.00	0.40	0.04	49.09	96.90	0.90	0.08	0.06	0.96	3
(2)	8	0.00	1.22	0.44	0.01	0.00	45.58	0.00	0.44	0.02	49.17	96.89	0.00	1.22	0.44	0.01	0.00	41.60	4.42	0.00	0.44	0.02	49.17	97.32	0.90	0.09	0.07	0.95	3
	9	0.00	1.06	0.46	0.00	0.00	45.51	0.00	0.45	0.05	49.22	96.76	0.00	1.06	0.46	0.00	0.00	41.92	3.99	0.00	0.45	0.05	49.22	97.15	0.91	0.08	0.06	0.96	3
	10	0.00	1.21	0.47	0.00	0.05	46.22	0.00	0.39	0.00	49.42	97.76	0.00	1.21	0.47	0.00	0.05	41.79	4.92	0.00	0.39	0.00	49.42	98.25	0.89	0.09	0.07	0.95	3
	11	0.00	1.19	0.53	0.02	0.03	45.45	0.00	0.38	0.01	49.46	97.07	0.00	1.19	0.53	0.02	0.03	41.79	4.07	0.00	0.38	0.01	49.46	97.48	0.90	0.08	0.07	0.96	3
	12	0.00	1.25	0.46	0.00	0.01	45.47	0.01	0.46	0.03	49.68	97.37	0.00	1.25	0.46	0.00	0.01	41.98	3.88	0.01	0.46	0.03	49.68	97.75	0.90	0.07	0.07	0.96	3
	13	0.00	1.34	0.44	0.00	0.01	42.31	0.01	0.47	0.02	50.78	95.37	0.00	1.34	0.44	0.00	0.01	42.31	0.00	0.01	0.47	0.02	50.78	95.37	0.93	0.00	0.07	1.00	3
	14	0.03	0.99	0.44	0.04	0.06	39.75	0.01	0.37	0.04	50.88	92.59	0.03	0.99	0.44	0.04	0.06	39.75	0.00	0.01	0.37	0.04	50.88	92.59	0.90	0.00	0.06	1.04	3
	1	0.00	1.40	0.62	0.00	0.09	47.63	0.03	0.37	0.00	50.48	100.63	0.00	1.40	0.62	0.00	0.09	42.21	6.03	0.03	0.37	0.00	50.48	101.24	0.87	0.11	0.08	0.94	3
	2	0.00	1.28	0.56	0.00	0.02	46.97	0.00	0.47	0.03	50.60	99.94	0.00	1.28	0.56	0.00	0.02	42.64	4.81	0.00	0.47	0.03	50.60	100.42	0.89	0.09	0.07	0.95	3
Fig. 2	3	0.00	1.30	0.54	0.01	0.04	47.06	0.01	0.45	0.03	50.64	100.09	0.00	1.30	0.54	0.01	0.04	42.65	4.91	0.01	0.45	0.03	50.64	100.58	0.89	0.09	0.07	0.95	3
(3)	4	0.00	1.31	0.56	0.03	0.00	47.38	0.04	0.42	0.02	50.91	100.66	0.00	1.31	0.56	0.03	0.00	42.86	5.02	0.04	0.42	0.02	50.91	101.16	0.89	0.09	0.07	0.95	3
	5	0.00	1.25	0.52	0.00	0.15	46.86	0.00	0.44	0.01	51.00	100.22	0.00	1.25	0.52	0.00	0.15	43.00	4.28	0.00	0.44	0.01	51.00	100.65	0.90	0.08	0.07	0.96	3
	6	0.00	1.36	0.64	0.01	0.12	46.74	0.00	0.38	0.09	51.05	100.39	0.00	1.36	0.64	0.01	0.12	42.72	4.46	0.00	0.38	0.09	51.05	100.84	0.89	0.08	0.08	0.95	3
	7	0.00	1.32	0.54	0.01	0.02	47.73	0.01	0.41	0.03	51.33	101.40	0.00	1.32	0.54	0.01	0.02	43.26	4.97	0.01	0.41	0.03	51.33	101.90	0.89	0.09	0.07	0.95	3
	1	0.00	1.32	0.43	0.00	0.06	45.34	0.03	0.47	0.00	49.24	96.88	0.00	1.32	0.43	0.00	0.06	41.46	4.32	0.03	0.47	0.00	49.24	97.31	0.89	0.08	0.07	0.95	3
Fig. 2	2	0.00	1.41	0.49	0.00	0.08	44.84	0.00	0.53	0.00	49.41	96.75	0.00	1.41	0.49	0.00	0.08	41.36	3.86	0.00	0.53	0.00	49.41	97.14	0.89	0.07	0.08	0.96	3
(4)	3	0.00	1.40	0.45	0.00	0.05	44.92	0.02	0.51	0.02	49.42	96.78	0.00	1.40	0.45	0.00	0.05	41.45	3.85	0.02	0.51	0.02	49.42	97.16	0.89	0.07	0.08	0.96	3
	4	0.00	1.37	0.47	0.02	0.06	44.94	0.03	0.47	0.01	49.44	96.81	0.00	1.37	0.47	0.02	0.06	41.48	3.85	0.03	0.47	0.01	49.44	97.19	0.89	0.07	0.08	0.96	3
	5	0.00	1.40	0.45	0.01	0.05	45.48	0.04	0.44	0.00	49.93	97.80	0.00	1.40	0.45	0.01	0.05	41.91	3.97	0.04	0.44	0.00	49.93	98.19	0.89	0.08	0.08	0.96	3
	1	0.06	0.64	0.47	0.01	0.00	46.44	0.00	0.42	0.00	45.77	93.82	0.06	0.64	0.47	0.01	0.00	39.61	7.58	0.00	0.42	0.00	45.77	94.57	0.88	0.15	0.05	0.92	3
	2	0.00	1.24	0.42	0.02	0.07	46.84	0.05	0.48	0.01	48.83	97.95	0.00	1.24	0.42	0.02	0.07	41.20	6.27	0.05	0.48	0.01	48.83	98.58	0.88	0.12	0.07	0.93	3
Fig. 2	3	0.00	1.21	0.43	0.02	0.00	47.19	0.04	0.46	0.00	48.89	98.24	0.00	1.21	0.43	0.02	0.00	41.35	6.49	0.04	0.46	0.00	48.89	98.88	0.88	0.12	0.07	0.93	3
(5)	4	0.00	1.28	0.44	0.00	0.00	46.41	0.02	0.42	0.00	49.01	97.58	0.00	1.28	0.44	0.00	0.00	41.36	5.61	0.02	0.42	0.00	49.01	98.14	0.88	0.11	0.07	0.94	3
	5	0.01	1.32	0.53	0.00	0.02	46.18	0.02	0.47	0.03	49.40	97.98	0.01	1.32	0.53	0.00	0.02	41.53	5.17	0.02	0.47	0.03	49.40	98.50	0.88	0.10	0.07	0.95	3
	6	0.00	1.28	0.48	0.00	0.04	46.31	0.02	0.39	0.05	49.74	98.32	0.00	1.28	0.48	0.00	0.04	41.94	4.85	0.02	0.39	0.05	49.74	98.80	0.89	0.09	0.07	0.95	3
	7	0.07	1.06	0.42	0.02	0.04	41.66	0.02	0.41	0.03	46.29	90.03	0.07	1.06	0.42	0.02	0.04	39.34	2.58	0.02	0.41	0.03	46.29	90.28	0.91	0.05	0.07	0.97	3
	1	0.00	1.63	0.54	0.02	0.10	45.60	0.00	0.53	0.01	49.28	97.70	0.00	1.63	0.54	0.02	0.10	40.76	5.37	0.00	0.53	0.01	49.28	98.24	0.87	0.10	0.09	0.94	3
	2	0.00	1.65	0.49	0.01	0.03	45.67	0.02	0.54	0.02	49.45	97.88	0.00	1.65	0.49	0.01	0.03	41.01	5.18	0.02	0.54	0.02	49.45	98.39	0.87	0.10	0.09	0.94	3
Fig. 2	3	0.00	1.61	0.48	0.00	0.12	45.32	0.03	0.52	0.02	49.84	97.93	0.00	1.61	0.48	0.00	0.12	41.37	4.38	0.03	0.52	0.02	49.84	98.37	0.88	0.08	0.09	0.95	3
(6)	4	0.00	1.62	0.58	0.00	0.02	45.31	0.03	0.50	0.00	49.87	97.93	0.00	1.62	0.58	0.00	0.02	41.37	4.38	0.03	0.50	0.00	49.87	98.37	0.88	0.08	0.09	0.95	3
	5	0.00	1.65	0.53	0.03	0.15	45.44	0.04	0.53	0.04	49.92	98.33	0.00	1.65	0.53	0.03	0.15	41.26	4.64	0.04	0.53	0.04	49.92	98.79	0.87	0.09	0.09	0.95	3
	6	0.00	1.59	0.47	0.02	0.06	45.70	0.03	0.47	0.01	50.00	98.35	0.00	1.59	0.47	0.02	0.06	41.60	4.56	0.03	0.47	0.01	50.00	98.80	0.88	0.09	0.08	0.95	3
	7	0.00	1.54	0.53	0.02	0.00	45.12	0.07	0.49	0.00	50.12	97.90	0.00	1.54	0.53	0.02	0.00	41.78	3.71	0.07	0.49	0.00	50.12	98.27	0.89	0.07	0.08	0.96	3
	8	1.29	0.24	1.05	0.11	0.08	31.44	1.18	0.44	0.06	57.95	93.83																	
Fig. 2	1	0.00	3.01	0.51	0.01	0.14	43.85	0.13	0.45	0.03	49.42	97.54	0.00	3.01	0.51	0.01	0.14	38.44	6.01	0.13	0.45	0.03	49.42	98.13	0.81	0.11	0.14	0.94	3
(7)	2	0.00	3.07	0.53	0.03	0.01	43.89	0.09	0.51	0.04	49.90	98.07	0.00	3.07	0.53	0.03	0.01	38.83	5.62	0.09	0.51	0.04	49.90	98.63	0.81	0.11	0.14	0.94	3
	1	0.00	3.39	1.01	0.02	0.02	50.67	0.22	0.33	0.10	41.49	97.24	0.00	3.39	1.01	0.02	0.02	30.22	22.72	0.22	0.33	0.10	41.49	99.51	0.63	0.43	0.18	0.78	3
	2	0.00	3.39	1.00	0.01	0.05	50.94	0.21	0.28	0.00	41.72	97.60	0.00	3.39	1.00	0.01	0.05	30.43	22.79	0.21	0.28	0.00	41.72	99.87	0.63	0.43	0.17	0.78	3
Fig. 2	3	0.00	3.50	1.02	0.02	0.11	50.69	0.25	0.31	0.01	41.74	97.65	0.00	3.50	1.02	0.02	0.11	30.16	22.81	0.25	0.31	0.01	41.74	99.93	0.63	0.43	0.18	0.78	3
(8)	4	0.00	3.48	1.05	0.02	0.09	50.68	0.25	0.29	0.03	41.89	97.76	0.00	3.48	1.05	0.02	0.09	30.32	22.62	0.25	0.29	0.03	41.89	100.02	0.63	0.42	0.18	0.78	3
	5	0.00	3.50	1.05	0.01	0.11	50.84	0.23	0.36	0.00	41.99	98.09	0.00	3.50	1.05	0.01	0.11	30.36	22.75	0.23	0.36	0.00	41.99	100.36	0.63	0.42	0.18	0.78	3
	6	0.00	3.57	1.00	0.00	0.09	50.68	0.23	0.23	0.10	42.06	97.96	0.00	3.57	1.00	0.00	0.09	30.39	22.54	0.23	0.23	0.10	42.06	100.21	0.63	0.42	0.18	0.78	3
	7	0.00	3.38	1.07	0.00	0.06	50.92	0.20	0.25	0.00	42.08	97.96	0.00	3.38	1.07	0.00	0.06	30.69	22.47	0.20	0.25	0.00	42.08	100.21	0.64	0.42	0.17	0.78	3
	1	0.00	4.05	0.54	0.03	0.10	44.45	0.28	0.61	0.08	49.45	99.58	0.00	4.05	0.54	0.03	0.10	36.60	8.72	0.28	0.61	0.08	49.45	100.45	0.75	0.16	0.19	0.91	3
Fig. 2	2	0.00	3.81	0.46	0.02	0.01	44.50	0.21	0.64	0.06	50.24	99.95	0.00	3.81	0.46	0.02	0.01	37.90	7.33	0.21	0.64	0.06	50.24	100.68	0.77	0.13	0.17	0.92	3
(9)	3	0.00	4.03	0.58	0.01	0.08	45.06	0.23	0.61	0.11	50.29	101.00	0.00	4.03	0.58	0.01	0.08	37.39	8.52	0.23	0.61	0.11	50.29	101.85	0.75	0.15	0.18	0.91	3

Grains	Spots	SiO_2	MgO	MnO	CaO	ZnO	FeO	Al_2O_3	V_2O_3	Cr_2O_3	TiO_2	Total	SiO_2	MgO	MnO	CaO	ZnO	FeO	Fe_2O_3	Al_2O_3	V_2O_3	Cr_2O_3	TiO_2	Total	Fe ferrous	Fe ferric	Other cations	Ti	O
Fig. 2 (10)	1	0.00	4.38	0.35	0.00	0.00	49.44	0.18	0.47	0.19	42.85	97.86	0.00	4.38	0.35	0.00	0.00	30.39	21.16	0.18	0.47	0.19	42.85	99.97	0.63	0.39	0.20	0.79	3
	2	0.00	4.51	0.37	0.01	0.04	49.76	0.26	0.50	0.11	42.88	98.43	0.00	4.51	0.37	0.01	0.04	30.13	21.81	0.26	0.50	0.11	42.88	100.61	0.62	0.40	0.21	0.79	3
	3	0.00	4.62	0.37	0.00	0.00	49.45	0.20	0.49	0.17	42.92	98.23	0.00	4.62	0.37	0.00	0.00	30.00	21.62	0.20	0.49	0.17	42.92	100.39	0.61	0.40	0.21	0.79	3
	4	0.00	4.65	0.37	0.00	0.12	49.71	0.22	0.47	0.17	42.94	98.64	0.00	4.65	0.37	0.00	0.12	29.86	22.05	0.22	0.47	0.17	42.94	100.85	0.61	0.40	0.21	0.79	3
	5	0.00	4.45	0.40	0.01	0.00	49.54	0.19	0.51	0.17	43.01	98.27	0.00	4.45	0.40	0.01	0.00	30.35	21.32	0.19	0.51	0.17	43.01	100.40	0.62	0.39	0.20	0.79	3
	6	0.00	4.46	0.35	0.01	0.20	49.21	0.21	0.46	0.15	43.13	98.18	0.00	4.46	0.35	0.01	0.20	30.30	21.01	0.21	0.46	0.15	43.13	100.28	0.62	0.39	0.21	0.80	3
Fig. 2 (11)	1	0.00	5.46	0.34	0.01	0.13	43.43	0.44	0.60	1.08	44.65	96.13	0.00	5.46	0.34	0.01	0.13	29.97	14.95	0.44	0.60	1.08	44.65	97.62	0.62	0.28	0.27	0.84	3
	2	0.00	5.41	0.37	0.00	0.01	43.40	0.45	0.59	1.04	44.66	95.92	0.00	5.41	0.37	0.00	0.01	30.14	14.73	0.45	0.59	1.04	44.66	97.39	0.63	0.28	0.27	0.84	3
	3	0.00	5.53	0.41	0.02	0.00	43.66	0.44	0.58	1.05	44.72	96.40	0.00	5.53	0.41	0.02	0.00	29.93	15.25	0.44	0.58	1.05	44.72	97.92	0.62	0.28	0.27	0.84	3
	4	0.00	5.56	0.38	0.02	0.12	42.96	0.46	0.61	1.16	44.82	96.07	0.00	5.56	0.38	0.02	0.12	29.90	14.52	0.46	0.61	1.16	44.82	97.52	0.62	0.27	0.28	0.84	3
	5	0.01	5.45	0.42	0.00	0.13	43.49	0.39	0.50	1.21	44.90	96.50	0.01	5.45	0.42	0.00	0.13	30.15	14.82	0.39	0.50	1.21	44.90	97.98	0.63	0.28	0.27	0.84	3
Fig. 2 (12)	1	0.07	4.99	0.44	0.00	0.06	44.07	0.57	0.46	0.26	46.65	97.58	0.07	4.99	0.44	0.00	0.06	32.65	12.68	0.57	0.46	0.26	46.65	98.84	0.67	0.24	0.24	0.87	3
	2	0.00	6.01	0.41	0.01	0.02	44.18	0.41	0.47	0.19	46.86	98.54	0.00	6.01	0.41	0.01	0.02	31.00	14.65	0.41	0.47	0.19	46.86	100.01	0.63	0.27	0.26	0.85	3
	3	0.00	6.60	0.48	0.01	0.15	43.23	0.23	0.48	0.25	47.19	98.62	0.00	6.60	0.48	0.01	0.15	30.06	14.63	0.23	0.48	0.25	47.19	100.08	0.61	0.27	0.28	0.86	3
	4	0.00	4.66	0.42	0.00	0.02	43.83	0.61	0.60	0.24	47.65	98.02	0.00	4.66	0.42	0.00	0.02	34.12	10.79	0.61	0.60	0.24	47.65	99.10	0.70	0.20	0.22	0.88	3
	5	0.10	4.57	0.41	0.02	0.05	42.85	0.65	0.56	0.31	47.69	97.21	0.10	4.57	0.41	0.02	0.05	34.39	9.40	0.65	0.56	0.31	47.69	98.15	0.71	0.18	0.22	0.89	3

However, in studying the Egyptian beach ilmenite of Rosetta and Damietta, the size and amount of the titanhematite exsolutions vary. Sometimes they are coarse, carrying fine exsolutions of ferriilmenite and forming up to 50% of the intergrowth. Occasionally they are too fine to be identified except under high magnification, and form less than 5% of the intergrowth [9]. In the present study, in most of the investigated titanhematite-ferriilmenite exsolution intergrowths, the exsolved titanhematite bodies occupy a minimum of 5% and up to 40% of the whole intergrowth. The majority of the grains exhibiting this intergrowth type have titanhematite exsolution bodies occupying about 10 - 20% of the whole intergrowth.

In some titanhematite-feiriilmenite exsolved intergrown grains, the ferriilmenite component may be altered into rutile and hematite (Figure 4 (5)-(6) and Figure 5 (7)). The alteration of ilmenite to rutile and hematite is generally attributed to oxidation [34]. Authors in [36] demonstrated experimentally that on heating pure ilmenite in air at 730^{o}C, it was completely oxidized into rutile and hematite with a very minor amount of brookite, but on further heating to 900^{o}C, a mixture of rutile and pseudobrookite was formed. Similar textures have been described from highly metamorphosed epidiorite from Assynt [37]. Subgraphic intergrowth of rutile and hematite with a thin outer rim of unaltered homogeneous ilmenite of Abu Ghalaga ilmenite ore was described in [34]

In the investigated samples, the ferriilmenite lamellae were found to be occasionally either partially or completely altered into rutile and hematite. In the concentrate under examination, some minor composite grains were detected, each of them consisting of two components. The first component is titanhematite bodies in ferriilmenite, whereas the second is feirilmenite in titanhematite (Figure 5 (8)-(9)). Several interpretations have been given to explain the different types of the titanhematite-ferriilmenite exsolution intergrowths [9, 22, 38]. Authors in [36] found that at normal temperatures, ferriilmenites with 18% Fe_20_3 and titanhemtites with 10% TiO_2 in solid solution exist in nature. According to [39], the unmixing of ilmenite and hematite from their solid solution takes place in two stages, the smaller bodies representing a "generation II" of exsolution formed at lower temperatures whereas the earlier and relatively coarser ones were termed as "generation I". According to [39], a gap in the miscibility range between Fe_2O_3 and $FeTiO_3$ originates below 600^{o}C, in which the solid solution splits into Fe_2O_3 bearing ilmenite and $FeTiO_3$ bearing hematite. With further temperature fall, the dissolving power of Fe_2O_3 in $FeTiO_3$ and of $FeTiO_3$ in Fe_2O_3 decreases intermittently and second generation exsolution discs are formed.

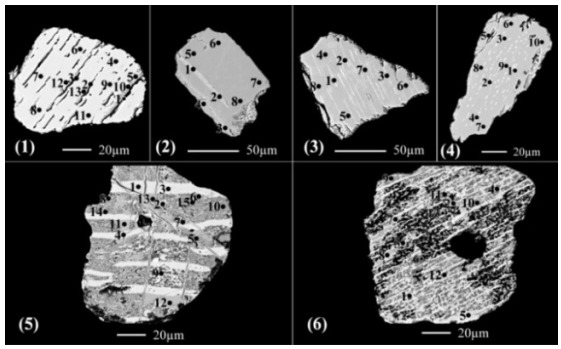

Fig. 4. BSE images of various detected titanhematites-ferriilmenites exsolved intergrowth grains.

The size of the exsolutions and the composition of the two components of the intergrowth depends on the rate of cooling, the original composition of the solid solution and the presence or absence of foreign oxides, such as MgO, MnO and Al_2O_3 [36]. The irregularity of some exsolution bodies indicates that they have grown in situ, by absorbing exsolution hematite in adjacent ferriilmenite [40]. Many of the larger exsolution lamellae are observed to have coalesced and are frequently irregular. Some of the coarse titanhematite exsolution bodies have a narrow rim of homogeneous ilmenite and seem to have grown in situ by diffusion [34]. In the present work, most of the observations given by [34, 40] were also detected. However, there are some reasons to accept the suggestion of the two generations given by [39] rather than others. These are :

- Some host ferriilmenite grains contain only one generation of the oriented titanhematite exsolutions.
- Some host ferriilmenite grains contain fine titanhematite exsolution bodies irregularly distributed without definite orientation.
- The presence of the composite grains is considered the most important factor to accept the suggestion of [39]. In these grains, any individual component, either of the ferriilmenite host or of the titanhematite host, could be itself considered as a first generation of exsolution due to the unmixing of 2 solid solutions, 1 of them composed mainly of ferriilmenite and the other mainly of titanhematite, derived from an original single solution. The relative percentages of the obtained 2 solid solutions are related to the concentrations of their corresponding essential components in the original solid solution, the temperature, and the rate of cooling. At a relatively lower temperature and definite rate of cooling, each individual component (e.g. ferriilmenite) exsolves some or most of the miscible hematite inside it. The same process could also occur for the second individual component, the titanhematite, where some or most of the miscible ilmenites are exsolved with the result of a second generation, in relation to the whole composite grain, of relatively much smaller exsolution bodies in each individual component.

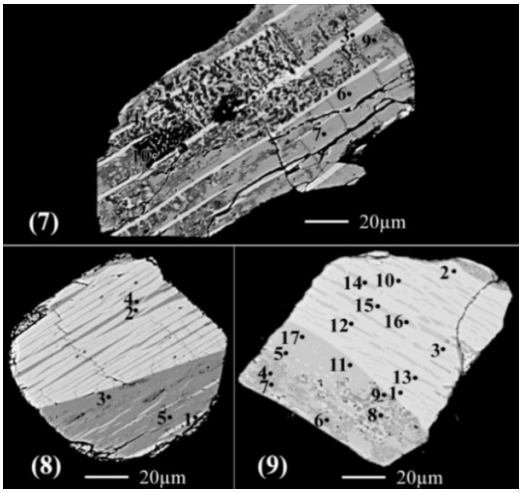

Fig. 5. BSE images of detected titanhematites-ferriilmenites exsolved intergrowth grains. In grain (7), the ferriilmenite component is altered into rutile and hematite. Composite grains (8)-(9) consist of two components, one being ferriilmenite- titanhematite and the other titanhematite-ferriilmenite.

After investigating the results of microprobe analysis of the various detected grains of hematite–ilmenite exsolution intergrowths contained in Figures 4-5, the following remarks can be noted. In Figure 4 (1) (Tables III-IV), spots 1-4 have considerable amounts of FeO oxidized into Fe_2O_3 which is partially leached and the remaining may have changed into goethite and/or hydrated iron oxides (Table III). In these spots, the SiO_2, Al_2O_3, and CaO contents are relatively higher. These impurity oxides may be phases carrying molecular and/or structural water, or they are associated with the molecular water necessary for the process of oxidation and hydroxylation of ferrous iron to ferric iron. So, the loaded impurity oxides are precipitated inside fissures. When this process of entering molecular water is repeated, bearing for these impurity oxides into fissures, an enrichment of the 3 impurity oxides occurs. Spots 6-9 and 11 are ferriilmenites where the Fe_2O_3 content ranges between 6.87 and 8.96% while the TiO_2 content ranges between 47.43 and 47.95%. In spots 5, 10, 12, and 13 some of of Fe_2O_3 content is lost from the ferriilmenite component adjacent to the altered titanhematite component. Their areas contain voids and molecular and/or structural water. Hence, the Fe_2O_3 content is decreased from 5% in spot 5 to 1.07% in spot 13. On the other hand, the content of TiO_2 is increased from 47.13% in spot 5 to 49.63% in spot 13, while the content of FeO is increased from 38.01% in spot 5 to 40.78% in spot 13.

In grain (2) of Figure 4, spots 1, 2 are titanhematite. The Fe_2O_3 content ranges between 55.47 and 60.21%, the TiO_2 content ranges between 19.22 and 22.4%, and the FeO content ranges between 14.18 and 16.69%. Spots 3-8 are ferriilmenite. The Fe_2O_3 content ranges between 6.09 and 8.54%. When comparing the contents of Al_2O_3, V_2O_3, and Cr_2O_3 of spots 1, 2 with those of spots 3-8, it is obvious that these oxides are correlated positively with Fe_2O_3 rather than with TiO_2. MnO and MgO are correlated positively with FeO and Fe_2O_3, but both favor FeO rather than Fe_2O_3. Spots 1-3 of grain (3) of Figure 4 are titanhematite with a maximum value of TiO_2 equal to 30.88%, which corresponds to 26.46% of FeO in spot 3. Spots 4-8 are almost ilmenites. The Fe_2O_3 content in these spots ranges between only 0.02 and 0.54%. When comparing the MgO and MnO contents of spots 1-3 with those of spots 4-8, it is obvious that they follow iron (Fe^{2+}, Fe^{3+}), but much more Fe^{2+} than Fe^{3+}. On the other hand, both Cr^{3+} and V^{3+} follow Fe^{3+} more than Fe^{2+} or Ti^{4+}. Spots 1-4 in grain (4), are titanhematite. The maximum value of TiO_2 is 16.34% which is correlated to the 13.71% of FeO. Spots 6-10 are ferriilmenite, with Fe_2O_3 ranging between 0.47 and 2.36%. When comparing the MnO, MgO, and Cr_2O_3 contents of spots 1-4 to spots 5-10, it is notable that MnO and MgO follow Fe^{2+} rather than Fe^{3+}, while Cr_2O_3 follows Fe^{3+} rather than Fe^{2+}. Spot 5 is in a crack, with most Fe_2O_3 being leached out while the SiO_2 content is enriched. In this spot, there is a considerable amount of molecular and/or structural water and all the remaining iron is ferrous iron. Spots 1-3 of grain (5), (Figure 4, Tables III-IV) are titanhematite, containing small bodies of exsolved ilmenite. In these spots, it is obvious that the content of Cr_2O_3 is relatively higher, reflecting the positive correlation between Cr_2O_3 and Fe_2O_3. Spots 4-9 are ferriilmenite and spots 5-9 altered to rutile and hematite with a considerable amount of molecular water, especially spots 6, 7. Spots 10-13 are ferriilmenite. In these spots, MgO and MnO are positively correlated with FeO, while Cr_2O_3 seems to vary inversely with FeO. Cr_2O_3 follows Fe_2O_3 rather than FeO. Comparing the contents of V_2O_5 in these 4 spots with those of the spots 1-4 or 5-9 reflects the positive correlation between V^{3+} with either Fe^{3+} and/or Ti^{4+} rather than Fe^{2+}. Therefore, V_2O_3 content is relatively higher in spots 1-4 which have relatively higher Fe_2O_3 content and also are relatively higher in spots 5-9 which have relatively higher TiO_2 content (Table III). In spots 14 and 15, some of the Fe_2O_3 associated with the ferriilmenite leached, resulting to increased TiO_2 content in these spots.

TABLE II. MICROPROBE CHEMICAL ANALYSES AND CORRESPONDING MOLECULAR FORMULAE OF THE ANALYZED SPOTS OF HOMOGENEOUS ILMENITE GRAINS WITH A RELATIVELY HIGHER Mn CONTENT. GRAINS (1)-(6) OF FIGURE 3

Grains	Spots	SiO_2	MgO	MnO	CaO	ZnO	FeO	Al_2O_3	V_2O_3	Cr_2O_3	TiO_2	Total	SiO_2	MgO	MnO	CaO	ZnO	FeO	Fe_2O_3	Al_2O_3	V_2O_3	Cr_2O_3	TiO_2	Total	Ferrous Fe	Ferric Fe	Other cations	Ti	O
Fig. 3 (1)	1	1.00	0.06	0.40	0.13	0.06	41.84	0.00	0.32	0.04	50.10	93.95	1.00	0.06	0.40	0.13	0.06	41.80	0.00	0.00	0.32	0.04	50.10	93.95	0.94	0.00	0.05	1.01	3
	2	0.00	0.16	0.45	0.01	0.05	45.04	0.00	0.33	0.01	52.19	98.22	0.00	0.16	0.45	0.01	0.05	45.00	0.00	0.00	0.33	0.01	52.19	98.22	0.97	0.00	0.02	1.01	3
	3	0.00	0.15	0.44	0.00	0.10	45.53	0.00	0.31	0.03	52.27	98.83	0.00	0.15	0.44	0.00	0.10	45.53	0.00	0.00	0.31	0.03	52.27	98.83	0.98	0.00	0.02	1.00	3
	4	0.00	0.15	0.45	0.00	0.03	45.20	0.00	0.38	0.04	52.30	98.56	0.00	0.15	0.45	0.00	0.03	45.20	0.00	0.00	0.38	0.04	52.30	98.56	0.97	0.00	0.02	1.01	3
	5	0.00	0.12	0.50	0.02	0.06	45.22	0.00	0.33	0.05	52.31	98.60	0.00	0.12	0.50	0.02	0.06	45.22	0.00	0.00	0.33	0.05	52.31	98.60	0.97	0.00	0.02	1.01	3
	6	0.00	0.16	0.47	0.01	0.06	45.53	0.00	0.44	0.01	52.36	99.04	0.00	0.16	0.47	0.01	0.06	45.53	0.00	0.00	0.44	0.01	52.36	99.04	0.97	0.00	0.03	1.00	3
	7	0.00	0.13	0.48	0.02	0.13	45.65	0.00	0.39	0.02	52.61	99.43	0.00	0.13	0.48	0.02	0.13	45.65	0.00	0.00	0.39	0.02	52.61	99.43	0.97	0.00	0.03	1.00	3
	8	0.00	0.13	0.42	0.00	0.05	45.04	0.00	0.36	0.01	52.66	98.68	0.00	0.13	0.42	0.00	0.05	45.04	0.00	0.00	0.36	0.01	52.66	98.68	0.97	0.00	0.02	1.01	3
	9	0.00	0.14	0.51	0.00	0.04	44.53	0.00	0.39	0.08	52.68	98.37	0.00	0.14	0.51	0.00	0.04	44.53	0.00	0.00	0.39	0.08	52.68	98.37	0.96	0.00	0.03	1.02	3
	10	0.05	0.15	0.36	0.07	0.00	35.24	0.02	0.42	0.03	57.14	93.50																	
Fig. 3 (2)	1	0.00	0.11	0.82	0.03	0.00	46.14	0.00	0.38	0.00	50.80	98.27	0.00	0.11	0.82	0.03	0.00	44.64	1.66	0.00	0.38	0.00	50.80	98.43	0.96	0.03	0.03	0.98	3
	2	0.00	0.06	0.87	0.02	0.04	46.03	0.00	0.39	0.04	50.83	98.28	0.00	0.06	0.87	0.02	0.04	44.67	1.51	0.00	0.39	0.04	50.83	98.43	0.96	0.03	0.03	0.98	3
	3	0.02	0.11	0.94	0.01	0.04	46.28	0.00	0.31	0.03	50.97	98.70	0.02	0.11	0.94	0.01	0.04	44.67	1.79	0.00	0.31	0.03	50.97	98.88	0.95	0.03	0.03	0.98	3
	4	0.00	0.08	0.82	0.00	0.05	45.50	0.00	0.47	0.02	51.11	98.04	0.00	0.08	0.82	0.00	0.05	44.97	0.59	0.00	0.47	0.02	51.11	98.10	0.97	0.01	0.03	0.99	3
	5	0.00	0.08	0.79	0.01	0.00	45.17	0.00	0.35	0.06	51.19	97.66	0.00	0.08	0.79	0.01	0.00	45.09	0.09	0.00	0.35	0.06	51.19	97.66	0.97	0.00	0.03	0.99	3
	6	0.20	0.04	0.87	0.02	0.00	45.54	0.00	0.41	0.02	51.32	98.42	0.20	0.04	0.87	0.02	0.00	45.43	0.12	0.00	0.41	0.02	51.32	98.42	0.97	0.00	0.03	0.99	3
Fig. 3 (3)	1	0.00	0.14	1.28	0.01	0.09	43.55	0.00	0.42	0.00	52.56	98.04	0.00	0.14	1.28	0.01	0.09	43.55	0.00	0.00	0.42	0.00	52.56	98.04	0.93	0.00	0.04	1.02	3
	2	0.00	0.09	1.10	0.01	0.07	44.01	0.00	0.34	0.00	52.66	98.26	0.00	0.09	1.10	0.01	0.07	44.01	0.00	0.00	0.34	0.00	52.66	98.26	0.96	0.00	0.04	1.02	3
	3	0.00	0.09	1.23	0.00	0.08	44.74	0.00	0.32	0.00	52.76	99.23	0.00	0.09	1.23	0.00	0.08	44.74	0.00	0.00	0.32	0.00	52.76	99.23	0.95	0.00	0.04	1.01	3
	4	0.00	0.10	1.15	0.01	0.02	43.57	0.00	0.33	0.02	52.81	98.01	0.00	0.10	1.15	0.01	0.02	43.57	0.00	0.00	0.33	0.02	52.81	98.01	0.93	0.00	0.04	1.02	3
	5	0.00	0.12	1.01	0.00	0.11	43.03	0.00	0.38	0.01	52.85	97.51	0.00	0.12	1.01	0.00	0.11	43.03	0.00	0.00	0.38	0.01	52.85	97.51	0.93	0.00	0.04	1.03	3
	6	0.01	0.11	1.01	0.01	0.05	43.61	0.00	0.36	0.03	52.89	98.08	0.01	0.11	1.01	0.01	0.05	43.61	0.00	0.00	0.36	0.03	52.89	98.08	0.94	0.00	0.04	1.02	3
	7	0.00	0.14	1.26	0.00	0.00	43.17	0.00	0.34	0.00	52.93	97.84	0.00	0.14	1.26	0.00	0.00	43.17	0.00	0.00	0.34	0.00	52.93	97.84	0.94	0.00	0.04	1.03	3
	8	0.00	0.13	1.18	0.00	0.14	43.89	0.00	0.34	0.00	52.96	98.63	0.00	0.13	1.18	0.00	0.14	43.89	0.00	0.00	0.34	0.00	52.96	98.63	0.94	0.00	0.04	1.02	3
	9	0.00	0.14	1.15	0.00	0.17	43.74	0.00	0.38	0.03	52.98	98.60	0.00	0.14	1.15	0.00	0.17	43.74	0.00	0.00	0.38	0.03	52.98	98.60	0.94	0.00	0.04	1.02	3
	10	0.00	0.15	1.14	0.00	0.10	42.88	0.00	0.44	0.03	53.03	97.77	0.00	0.15	1.14	0.00	0.10	42.88	0.00	0.00	0.44	0.03	53.03	97.77	0.93	0.00	0.04	1.03	3
	11	0.00	0.17	1.15	0.01	0.13	43.16	0.00	0.40	0.00	53.10	98.12	0.00	0.17	1.15	0.01	0.13	43.16	0.00	0.00	0.40	0.00	53.10	98.12	0.93	0.00	0.04	1.03	3
	12	0.00	0.15	1.28	0.01	0.03	43.16	0.00	0.36	0.04	53.14	98.18	0.00	0.15	1.28	0.01	0.03	43.16	0.00	0.00	0.36	0.04	53.14	98.18	0.92	0.00	0.04	1.03	3
	13	0.00	0.15	1.26	0.02	0.03	42.91	0.00	0.39	0.00	53.21	97.97	0.00	0.15	1.26	0.02	0.03	42.91	0.00	0.00	0.39	0.00	53.21	97.97	0.93	0.00	0.04	1.03	3
Fig. 3 (4)	1	0.00	0.34	1.60	0.06	0.00	45.75	0.00	0.34	0.01	48.49	96.60	0.00	0.34	1.60	0.06	0.00	41.33	4.91	0.00	0.34	0.01	48.49	97.09	0.90	0.10	0.06	0.95	3
	2	0.00	0.26	1.69	0.07	0.05	45.86	0.00	0.30	0.00	48.79	97.02	0.00	0.26	1.69	0.07	0.05	41.60	4.74	0.00	0.30	0.00	48.79	97.49	0.90	0.09	0.06	0.95	3
	3	0.00	0.39	1.59	0.00	0.00	46.19	0.00	0.34	0.00	49.00	97.51	0.00	0.39	1.59	0.00	0.00	41.78	4.90	0.00	0.34	0.00	49.00	97.99	0.90	0.09	0.06	0.95	3
	4	0.00	0.35	1.70	0.01	0.03	46.18	0.00	0.29	0.00	49.03	97.59	0.00	0.35	1.70	0.01	0.03	41.71	4.96	0.00	0.29	0.00	49.03	98.08	0.90	0.10	0.06	0.95	3
	5	0.00	0.38	1.49	0.00	0.00	46.30	0.00	0.37	0.00	49.13	97.67	0.00	0.38	1.49	0.00	0.00	42.01	4.77	0.00	0.37	0.00	49.13	98.14	0.90	0.09	0.06	0.95	3
	6	0.00	0.36	1.68	0.03	0.05	45.04	0.00	0.36	0.00	49.72	97.23	0.00	0.36	1.68	0.03	0.05	42.31	3.03	0.00	0.36	0.00	49.72	97.53	0.91	0.06	0.06	0.97	3
Fig. 3 (5)	1	0.00	2.44	3.11	0.00	0.12	46.52	0.00	0.28	0.00	42.53	95.00	0.00	2.44	3.11	0.00	0.12	30.66	17.62	0.00	0.28	0.00	42.53	96.76	0.66	0.34	0.18	0.83	3
	2	0.00	2.48	3.27	0.00	0.25	46.50	0.00	0.32	0.00	42.54	95.36	0.00	2.48	3.27	0.00	0.25	30.31	17.98	0.00	0.32	0.00	42.54	97.15	0.65	0.35	0.19	0.82	3
	3	0.00	2.37	3.07	0.00	0.22	45.87	0.00	0.29	0.02	42.57	94.41	0.00	2.37	3.07	0.00	0.22	30.78	16.77	0.00	0.29	0.02	42.57	96.09	0.67	0.33	0.18	0.83	3
	4	0.00	2.37	3.46	0.00	0.06	46.62	0.00	0.33	0.00	42.61	95.45	0.00	2.37	3.46	0.00	0.06	30.56	17.85	0.00	0.33	0.00	42.61	97.23	0.66	0.35	0.18	0.82	3
	5	0.00	2.43	3.12	0.00	0.18	45.97	0.00	0.30	0.05	42.64	94.70	0.00	2.43	3.12	0.00	0.18	30.70	16.97	0.00	0.30	0.05	42.64	96.39	0.66	0.33	0.18	0.83	3
	6	0.00	2.52	3.27	0.00	0.18	46.71	0.02	0.32	0.02	42.75	95.80	0.00	2.52	3.27	0.00	0.18	30.51	18.01	0.02	0.32	0.02	42.75	97.59	0.65	0.35	0.19	0.82	3
	7	0.00	1.87	2.67	0.00	0.14	46.41	0.00	0.39	0.00	43.53	95.01	0.00	1.87	2.67	0.00	0.14	32.99	14.90	0.00	0.39	0.00	43.53	96.49	0.72	0.29	0.15	0.85	3
Fig. 3 (6)	1	2.39	0.19	5.42	0.15	0.15	39.95	0.09	0.49	0.06	42.76	91.65	2.39	0.19	5.42	0.15	0.15	35.18	5.30	0.09	0.49	0.06	42.76	92.18	0.80	0.11	0.22	0.87	3
	2	0.86	0.07	5.51	0.11	0.10	44.59	0.03	0.50	0.09	45.14	96.99	0.86	0.07	5.51	0.11	0.10	35.70	9.87	0.03	0.50	0.09	45.14	97.98	0.77	0.19	0.17	0.88	3
	3	0.50	0.16	5.88	0.09	0.01	39.15	0.02	0.42	0.08	45.67	91.96	0.50	0.16	5.88	0.09	0.01	35.32	4.25	0.02	0.42	0.08	45.67	92.39	0.81	0.09	0.17	0.94	3
	4	0.21	0.04	6.09	0.15	0.03	44.47	0.06	0.41	0.02	46.12	97.60	0.21	0.04	6.09	0.15	0.03	35.27	10.22	0.06	0.41	0.02	46.12	98.62	0.76	0.20	0.16	0.89	3
	5	0.42	0.10	6.09	0.08	0.08	39.21	0.02	0.45	0.00	46.20	92.65	0.42	0.10	6.09	0.08	0.08	35.54	4.08	0.02	0.45	0.00	46.20	93.06	0.81	0.08	0.17	0.94	3
	6	0.00	0.09	5.18	0.01	0.07	46.06	0.05	0.48	0.02	47.09	99.06	0.00	0.09	5.18	0.01	0.07	36.88	10.20	0.05	0.48	0.02	47.09	100.07	0.78	0.19	0.13	0.90	3
	7	0.00	0.09	4.53	0.00	0.05	46.42	0.09	0.52	0.05	47.15	98.89	0.00	0.09	4.53	0.00	0.05	37.63	9.77	0.09	0.52	0.05	47.15	99.87	0.80	0.19	0.12	0.90	3
	8	0.00	0.11	4.52	0.01	0.00	46.26	0.08	0.49	0.00	47.18	98.65	0.00	0.11	4.52	0.01	0.00	37.65	9.57	0.08	0.49	0.00	47.18	99.61	0.80	0.18	0.12	0.90	3
	9	0.33	0.07	5.18	0.08	0.01	40.65	0.01	0.44	0.02	47.43	94.22	0.33	0.07	5.18	0.08	0.01	37.58	3.41	0.01	0.44	0.02	47.43	94.56	0.84	0.07	0.14	0.95	3

Spots 1-5 of grain (6) of Figure 4 (Tables III, IV), are titanhematite. Spot 6 is titanhematite where a considerable amount of Fe_2O_3 is leached, resulting in the enrichment of TiO_2. In this spot, there is also a considerable amount of molecular water (Table III). Spots 7-8 are ferriilmenite associated with pyrophanite ($MnTiO_3$) in solid solution. The MnO content ranges between 6.36 and 6.64%. Spots 9-13 are ilmenite altered to rutile and hematite. The TiO_2 content ranges between 57.6 and 93.87%, while the Fe_2O_3 content ranges between 41.14 and 4.86%. As the Fe_2O_3 content decreases, the TiO_2 content increases and the sum of total analyzed oxides is around 100%. From the MnO content in these 5 spots, it is

obvious that most iron is ferric iron. Also, the back scattered electron image of grain (6) reflects that most of titanhematite associated with TiO_2 is leached out lefting voids of various sizes. Spots 1-5 of grain (7), of Figure 5 (Tables III, IV), are titanhematite with TiO_2 content ranging between 11.5 and 23.84%. Comparing the values of FeO with TiO_2 in spots 1-3 with those of spots 4-5 reflects that there is also an individual phase of TiO_2 in spots 4-5 associated with hematite and ilmenite in the titanhematite. Spots 6-8 are ferriilmenite associated with pyrophanite in solid solution. Maximum MnO content (8.58%) occurs in spot 8. Spots 9-10 are rutile and hematite where some of Fe_2O_3 is leached out, especially from spot 10. It is obvious from the investigation of spot 6 of grain (6) of Figure 4 and spot 10 of grain (7) of Figure 5, that the leaching mechanism of Fe_2O_3 is related to the activity of molecular water which seems to be either associated with dissolved silica or the water molecules or hydroxyl anions complexed with silica and each time the associated SiO_2 after losing its water content is precipitated in the cracks or pores and finally enriched (SiO_2 content equals to 9.17% in spot 10 of grain (7)). Some minor composite grains were detected, each of them composed of two parts. The first part is titanhematite exsolution bodies in ferriilmenite and the second part is feirilmenite exsolution in titanhematite. The contact between the two parts may be curved, irregular, or perfectly straight. In the majority of the composite grains, the part of the exsolved titanhematite in the host ferriilmenite is the essential one, and may represent up to 80% of the composite grain. On the other hand, in a few grains the part of exsolved ferriilmenite in the host titanhematite is the essential one and represents up to 60% of the composite grain. The composite grain (8) of Figure 5 (Tables III, IV) consists of 2 parts, the first part is relatively larger and consists of a ferriilmenite-titanhematite component, while the second part is relatively smaller and consists of a titanhematite-ferriilmenite component. Spots 1-2 are almost similar titanhematites, although they are not in the same part of the grain. Spots 3-5 are ferriilmenite. Also, with the exception of spot 4 in the ferriilmenite-titanhematite part and spots 3-5 in the titanhematite-ferriilmenite part, their chemical composition is almost the same. The result of the comparison of the chemical composition of titanhematite (spots 1, 2) and ferriilmenite (spots 3-5) is that MgO, MnO, and ZnO follow FeO and hence, are mixed with ilmenite rather than with hematite. However, Cr_2O_3, V_2O_3, and Al_2O_3 follow Fe^{3+} rather than Fe^{2+}.

Grain (9) of Figure 5 (Tables III, IV), consists of 2 parts. The first part is relatively larger and consists of a ferriilmenite-titanhematite component while the other part consists of a titanhematite-ferriilmenite component. Spots 1-5 are titanhematite inside a major ferriilmenite component. The TiO_2 content ranges between 9.02 and 17.5%. In these spots, the V_2O_3 content is relatively greater, which may reflect that V_2O_3 follows Fe_2O_3 rather than TiO_2 or FeO. Also, the MgO and MnO content of spots 1-5 indicates that they follow FeO rather than Fe_2O_3. Spots 6-7 are pseudorutile (psr) associated with definite amounts of structural and/or molecular water (Table III). The sums of total analyzed oxides after applying an adopted Excel psr formula for the two spots are 95.13 and 96%. The 2 major oxides, TiO_2 and Fe_2O_3 of each spot, are recalculated by multiplying with 100/95.13 for spot 6 and with 100/96 for spot 7, which gives the following results: 60.38% TiO_2 and 38.31% Fe_2O_3 for spot 6 and 61.01% TiO_2 and 36.9% Fe_2O_3 for spot 7. Spots 8-9 are leached pseudorutile (lpsr) of various phases. In spots 8-9, the alteration mechanism is different than in spots 6-7, where the calculated structural water by the adopted excel program is incorrect and/or some of the analyzed TiO_2 and/or Fe_2O_3 is not included in the lpsr chemical formula. Spots 10-17 are ferriilmenite with some dissolved individual TiO_2 phase especially in the spots 14-17. The MnO and MgO contents in ferriilmenite (spots 10-17) indicate that both oxides follow FeO rather than Fe_2O_3. Comparing the contents of V_2O_3 and Cr_2O_3 of titanhematite (spots 1-5) and ferriilmenite (spots 10-17), clearly shows that both oxides follow Fe_2O_3 rather than FeO. Comparing the V_2O_3 content in all the analyzed spots of grain (9) reflects that V_2O_3 follows Fe_2O_3 in spots 1-5 and TiO_2 in spots 10-17 (Table III).

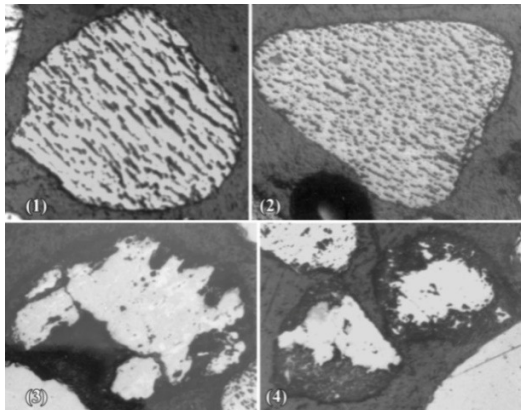

Fig. 6. Partially altered ilmenite grain textures: (1) Titanhematite-ferriilmenite exsolution intergrowth with most of the oriented exsolved titanhematite replaced by goethite or limonitic material. Reflected light, ×100. (2) Skeletal ilmenite grain with micropores arranged in a crystallographic orientation, indicating leaching out of hematite exsolution lamellae. Reflected light, ×100. (3) Subgraphic intergrowth of titanhematite and ferriilmenite components with isotropic leucoxenated material along the periphery of the grain and invading its inner part. Reflected light, ×100. (4) Two partially leucoxenated grains: the left grain shows an isotropic leucoxenated rim (black) completely surrounding the core of titanhematite-ferriilmenite subgraphic intergrowth. The right grain is an ilmenite grain (light grey) containing considerable leucoxenated areas (black) initiated on ilmenite parts originally replaced by sphene (dark grey). Reflected light, ×100.

C. Partially Altered Ilmenite (7.3%)

1) Leached Titanhematite Component (1.5%)

In a considerable number of the titanhematite-ferriilmenite exsolution intergrowthed grains, the host ferriilmenite contains micropores arranged in a crystallographic orientation pattern indicating the leaching out of hematite exsolution lamellae (Figure 6(1)-(2)). The size and shape of these micropores are related to those of the preexisting replaced hematite. The same texture was detected and the grains were called skeletal ilmenite grains [41] or pitted ilmenite [12]. The tendency of the hematite bodies to be more susceptable to this type of alteration than the ilmenite host is probably due to the fact that the free ferric oxide of hematite can be more easily hydrated than the ferrous oxide combined in the ilmenite structure. However, the original grain sizes may affect their rate of alteration [42].

TABLE III. MICROPROBE CHEMICAL ANALYSIS AND CORRESPONDING MOLECULAR FORMULAE OF THE ANALYZED SPOTS OF THE TITANHEMATITE-FERRIILMENITE GRAINS OF FIGURE 4(1)-(6) AND FIGURE 5(7)-(9)

Grains	Spots	SiO_2	MgO	MnO	CaO	ZnO	FeO	Al_2O_3	V_2O_3	Cr_2O_3	TiO_2	Total	SiO_2	MgO	MnO	CaO	ZnO	FeO	Fe_2O_3	Al_2O_3	V_2O_3	Cr_2O_3	TiO_2	Total	Ferrous Fe	Ferric Fe	Other cations	Ti	O
Fig. 4 (1)	1	3.09	2.30	0.40	0.12	0.07	42.05	0.59	0.54	0.04	39.59	88.79	3.09	2.30	0.40	0.12	0.07	34.59	8.28	0.59	0.54	0.04	39.59	89.62	0.79	0.17	0.23	0.81	3
	2	3.46	2.20	0.35	0.70	0.22	40.52	0.82	0.60	0.02	41.27	90.15	3.46	2.20	0.35	0.70	0.22	35.90	5.13	0.82	0.60	0.02	41.27	90.66	0.81	0.10	0.26	0.84	3
	3	1.82	2.34	0.43	0.16	0.07	40.89	0.92	0.60	0.00	41.74	88.96	1.82	2.34	0.43	0.16	0.07	34.85	6.71	0.92	0.60	0.00	41.74	89.63	0.80	0.14	0.21	0.86	3
	4	3.69	2.73	0.44	0.08	0.08	39.89	1.33	0.58	0.02	43.73	92.58	3.69	2.73	0.44	0.08	0.08	38.26	1.81	1.33	0.58	0.02	43.73	92.75	0.84	0.04	0.27	0.86	3
	5	0.12	2.33	0.33	0.02	0.02	42.51	0.06	0.51	0.06	47.13	93.09	0.12	2.33	0.33	0.02	0.02	38.01	5.00	0.06	0.51	0.06	47.13	93.58	0.84	0.10	0.12	0.94	3
	6	0.17	2.42	0.40	0.02	0.03	44.27	0.10	0.55	0.03	47.43	95.44	0.17	2.42	0.40	0.02	0.03	38.09	6.87	0.10	0.55	0.03	47.43	96.12	0.82	0.13	0.13	0.92	3
	7	0.00	2.57	0.43	0.03	0.13	45.63	0.06	0.56	0.00	47.51	96.93	0.00	2.57	0.43	0.03	0.13	37.57	8.96	0.06	0.56	0.00	47.51	97.82	0.80	0.17	0.13	0.91	3
	8	0.00	2.54	0.41	0.02	0.09	45.37	0.04	0.62	0.03	47.82	96.93	0.00	2.54	0.41	0.02	0.09	37.98	8.21	0.04	0.62	0.03	47.82	97.75	0.81	0.16	0.12	0.91	3
	9	0.00	2.52	0.38	0.05	0.06	46.01	0.09	0.55	0.00	47.88	97.54	0.00	2.52	0.38	0.05	0.06	38.07	8.82	0.09	0.55	0.00	47.88	98.41	0.80	0.17	0.12	0.91	3
	10	0.15	2.11	0.38	0.02	0.00	41.83	0.05	0.54	0.02	47.89	92.98	0.15	2.11	0.38	0.02	0.00	39.07	3.06	0.05	0.54	0.02	47.89	93.28	0.87	0.06	0.11	0.96	3
	11	0.00	2.52	0.47	0.00	0.07	45.77	0.08	0.60	0.01	47.95	97.49	0.00	2.52	0.47	0.00	0.07	38.10	8.53	0.08	0.60	0.01	47.95	98.34	0.80	0.16	0.12	0.91	3
	12	0.10	2.25	0.37	0.05	0.03	42.26	0.07	0.56	0.00	48.78	94.47	0.10	2.25	0.37	0.05	0.03	39.54	3.03	0.07	0.56	0.00	48.78	94.77	0.87	0.06	0.12	0.96	3
	13	0.16	2.01	0.36	0.06	0.04	41.75	0.07	0.58	0.02	49.63	94.68	0.16	2.01	0.36	0.06	0.04	40.78	1.07	0.07	0.58	0.02	49.63	94.78	0.89	0.02	0.11	0.98	3
Fig. 4 (2)	1	0.02	1.26	0.51	0.00	0.42	68.37	3.15	1.25	1.17	19.22	95.38	0.02	1.26	0.51	0.00	0.42	14.18	60.21	3.15	1.25	1.17	19.22	101.40	0.30	1.13	0.26	0.36	3
	2	0.02	1.51	0.44	0.03	0.35	66.62	2.99	1.18	1.06	22.40	96.59	0.02	1.51	0.44	0.03	0.35	16.69	55.47	2.99	1.18	1.06	22.40	102.13	0.35	1.03	0.25	0.42	3
	3	0.12	4.61	0.49	0.06	0.00	42.27	0.08	0.51	0.08	48.32	96.52	0.12	4.61	0.49	0.06	0.00	34.83	8.27	0.08	0.51	0.08	48.32	97.35	0.73	0.16	0.21	0.91	3
	4	0.20	4.26	0.54	0.09	0.08	43.38	0.12	0.49	0.10	48.66	97.91	0.20	4.26	0.54	0.09	0.08	35.69	8.54	0.12	0.49	0.10	48.66	98.76	0.74	0.16	0.20	0.91	3
	5	0.00	3.66	0.56	0.03	0.06	44.59	0.13	0.50	0.11	50.34	99.99	0.00	3.66	0.56	0.03	0.06	38.11	7.20	0.13	0.50	0.11	50.34	100.71	0.78	0.13	0.17	0.93	3
	6	0.00	3.59	0.61	0.02	0.08	44.09	0.11	0.58	0.15	50.45	99.67	0.00	3.59	0.61	0.02	0.08	38.26	6.47	0.11	0.58	0.15	50.45	100.32	0.79	0.12	0.17	0.93	3
	7	0.00	3.54	0.62	0.03	0.01	44.59	0.14	0.51	0.15	51.24	100.82	0.00	3.54	0.62	0.03	0.01	39.11	6.09	0.14	0.51	0.15	51.24	101.42	0.79	0.11	0.16	0.94	3
	8	0.00	3.74	0.55	0.01	0.00	44.74	0.09	0.56	0.13	51.34	101.15	0.00	3.74	0.55	0.01	0.00	38.96	6.42	0.09	0.56	0.13	51.34	101.79	0.79	0.12	0.17	0.93	3
Fig. 4 (3)	1	0.00	0.08	0.71	0.00	0.00	76.60	0.00	0.47	0.06	19.12	97.04	0.00	0.08	0.71	0.00	0.00	16.34	66.95	0.00	0.47	0.06	19.12	103.73	0.34	1.27	0.04	0.36	3
	2	0.00	0.08	0.71	0.00	0.00	75.41	0.00	0.44	0.07	20.94	97.64	0.00	0.08	0.71	0.00	0.00	17.99	63.79	0.00	0.44	0.07	20.94	104.01	0.38	1.20	0.03	0.39	3
	3	0.00	0.08	1.12	0.00	0.04	65.65	0.00	0.45	0.04	30.88	98.25	0.00	0.08	1.12	0.00	0.04	26.46	43.53	0.00	0.45	0.04	30.88	102.60	0.56	0.82	0.04	0.58	3
	4	0.00	0.12	1.89	0.01	0.00	45.03	0.00	0.35	0.00	51.92	99.31	0.00	0.12	1.89	0.01	0.00	44.56	0.51	0.00	0.35	0.00	51.92	99.36	0.95	0.01	0.05	0.99	3
	5	0.00	0.13	1.66	0.00	0.02	45.49	0.00	0.32	0.00	52.17	99.80	0.00	0.13	1.66	0.00	0.02	45.01	0.54	0.00	0.32	0.00	52.17	99.85	0.95	0.01	0.05	0.99	3
	6	0.00	0.17	1.86	0.01	0.10	44.76	0.00	0.42	0.01	52.20	99.52	0.00	0.17	1.86	0.01	0.10	44.69	0.08	0.00	0.42	0.01	52.20	99.52	0.95	0.00	0.06	0.99	3
	7	0.00	0.15	1.85	0.03	0.00	45.22	0.00	0.39	0.00	52.24	99.88	0.00	0.15	1.85	0.03	0.00	44.81	0.45	0.00	0.39	0.00	52.24	99.92	0.95	0.01	0.05	0.99	3
	8	0.00	0.11	1.73	0.00	0.00	45.20	0.00	0.37	0.01	52.40	99.84	0.00	0.11	1.73	0.00	0.00	45.18	0.02	0.00	0.37	0.01	52.40	99.84	0.95	0.00	0.05	1.00	3
Fig. 4 (4)	1	0.00	0.05	0.32	0.00	0.00	78.78	0.00	0.39	0.12	10.26	89.92	0.00	0.05	0.32	0.00	0.00	8.82	77.72	0.00	0.39	0.12	10.26	97.68	0.20	1.57	0.03	0.21	3
	2	0.00	0.04	0.36	0.02	0.00	78.08	0.00	0.39	0.08	10.62	89.59	0.00	0.04	0.36	0.02	0.00	9.09	76.65	0.00	0.39	0.08	10.62	97.25	0.21	1.56	0.03	0.22	3
	3	0.00	0.06	0.54	0.01	0.00	75.91	0.00	0.36	0.10	13.07	90.04	0.00	0.06	0.54	0.01	0.00	11.10	72.00	0.00	0.36	0.10	13.07	97.24	0.25	1.46	0.03	0.26	3
	4	0.00	0.05	0.85	0.02	0.02	73.16	0.00	0.35	0.08	16.34	90.87	0.00	0.05	0.85	0.02	0.02	13.71	66.06	0.00	0.35	0.08	16.34	97.47	0.31	1.33	0.04	0.33	3
	5	0.88	0.23	3.42	0.07	0.05	39.16	0.00	0.33	0.02	49.60	93.76	0.88	0.23	3.42	0.07	0.05	39.16	0.00	0.33	0.02	49.60	93.76	98.10	0.88	0.00	0.12	1.00	3
	6	0.00	0.28	3.50	0.00	0.00	43.23	0.00	0.34	0.00	50.18	97.53	0.00	0.28	3.50	0.00	0.00	41.10	2.36	0.00	0.34	0.00	50.18	97.76	0.89	0.05	0.09	0.97	3
	7	0.00	0.33	3.57	0.02	0.02	42.83	0.00	0.34	0.03	50.53	97.66	0.00	0.33	3.57	0.02	0.02	41.23	1.77	0.00	0.34	0.03	50.53	97.83	0.89	0.03	0.10	0.98	3
	8	0.00	0.35	3.58	0.04	0.21	42.79	0.00	0.32	0.01	50.54	97.83	0.00	0.35	3.58	0.04	0.21	40.98	2.01	0.00	0.32	0.01	50.54	98.03	0.88	0.04	0.10	0.98	3
	9	0.00	0.32	3.66	0.00	0.06	43.11	0.00	0.28	0.01	50.57	98.01	0.00	0.32	3.66	0.00	0.06	41.16	2.17	0.00	0.28	0.01	50.57	98.23	0.88	0.04	0.10	0.98	3
	10	0.00	0.24	3.69	0.00	0.00	42.39	0.00	0.33	0.07	51.29	98.02	0.00	0.24	3.69	0.00	0.00	41.97	0.47	0.00	0.33	0.07	51.29	98.07	0.90	0.01	0.10	0.99	3
Fig. 4 (5)	1	0.00	0.01	0.44	0.00	0.01	76.67	0.00	0.66	0.51	12.71	91.01	0.00	0.01	0.44	0.00	0.01	10.97	72.99	0.00	0.66	0.51	12.71	98.30	0.24	1.47	0.05	0.25	3
	2	0.00	0.05	0.49	0.01	0.14	76.30	0.00	0.56	0.44	12.73	90.73	0.00	0.05	0.49	0.01	0.14	10.72	72.86	0.00	0.56	0.44	12.73	98.00	0.24	1.47	0.05	0.26	3
	3	0.00	0.01	0.22	0.03	0.00	69.14	0.00	0.69	0.47	19.58	90.12	0.00	0.01	0.22	0.03	0.00	17.35	57.53	0.00	0.69	0.47	19.58	95.87	0.39	1.18	0.04	0.40	3
	4	0.00	0.00	0.06	0.03	0.00	59.61	0.00	0.63	0.48	32.00	92.81	0.00	0.00	0.06	0.03	0.00	28.69	34.36	0.00	0.63	0.48	32.00	96.25	0.64	0.69	0.03	0.64	3
	10	0.09	0.00	0.91	0.11	0.00	45.55	0.00	0.40	0.08	45.55	92.68	0.09	0.00	0.91	0.11	0.00	40.02	6.15	0.00	0.40	0.08	45.55	93.29	0.91	0.13	0.04	0.93	3
	11	0.05	0.11	6.22	0.06	0.11	43.81	0.00	0.34	0.08	46.29	97.05	0.05	0.11	6.22	0.06	0.11	35.04	9.73	0.00	0.34	0.08	46.29	98.02	0.76	0.19	0.16	0.90	3
	12	0.00	0.48	3.50	0.11	0.03	45.42	0.00	0.34	0.05	47.63	97.55	0.00	0.48	3.50	0.11	0.03	38.28	7.92	0.00	0.34	0.05	47.63	98.34	0.82	0.15	0.11	0.92	3
	13	0.00	0.47	4.19	0.00	0.08	44.11	0.00	0.41	0.05	48.27	97.58	0.00	0.47	4.19	0.00	0.08	38.27	6.49	0.00	0.41	0.05	48.27	98.23	0.82	0.13	0.12	0.93	3
	14	0.00	0.07	0.35	0.01	0.00	41.87	0.00	0.47	0.11	48.99	91.87	0.00	0.07	0.35	0.01	0.00	41.87	0.00	0.00	0.47	0.11	48.99	91.87	0.96	0.00	0.02	1.01	3
	15	0.02	0.34	2.20	0.05	0.03	38.35	0.00	0.46	0.16	51.28	92.87	0.02	0.34	2.20	0.05	0.03	38.35	0.00	0.00	0.46	0.16	51.28	92.87	0.88	0.00	0.08	1.05	3
Fig. 4 (6)	1	0.00	0.00	0.02	0.01	0.03	90.33	0.00	0.15	0.03	5.81	96.38	0.00	0.00	0.02	0.01	0.03	5.18	94.61	0.00	0.15	0.03	5.81	105.83	0.11	1.78	0.01	0.11	3
	2	0.03	0.00	0.26	0.01	0.06	85.87	0.00	0.13	0.07	7.90	94.32	0.03	0.00	0.26	0.01	0.06	6.81	87.84	0.00	0.13	0.07	7.90	103.10	0.15	1.69	0.02	0.15	3
	3	0.00	0.03	0.42	0.01	0.03	80.20	0.00	0.39	0.06	12.99	94.11	0.00	0.03	0.42	0.01	0.03	11.17	76.69	0.00	0.39	0.06	12.99	101.78	0.24	1.49	0.03	0.25	3
	4	0.00	0.03	0.57	0.00	0.00	79.06	0.00	0.43	0.12	13.66	93.86	0.00	0.03	0.57	0.00	0.00	11.65	74.89	0.00	0.43	0.12	13.66	101.34	0.25	1.46	0.03	0.27	3
	5	0.00	0.01	0.66	0.00	0.07	79.62	0.00	0.49	0.10	13.69	94.64	0.00	0.01	0.66	0.00	0.07	11.57	75.60	0.00	0.49	0.10	13.69	102.19	0.25	1.46	0.04	0.26	3
	6	3.31	0.17	0.34	0.12	0.07	44.02	0.02	0.45	0.10	40.11	88.72	3.31	0.17	0.34	0.12	0.07	39.19	5.37	0.02	0.45	0.10	40.11	89.26	0.92	0.11	0.13	0.84	3
	7	0.04	0.09	6.64	0.09	0.01	42.75	0.00	0.33	0.01	47.33	97.28	0.04	0.09	6.64	0.09	0.01	35.61	7.93	0.00	0.33	0.01	47.33	98.07	0.77	0.15	0.16	0.92	3
	8	0.00	0.04	6.36	0.01	0.10	44.81	0.00	0.37	0.02	48.46	100.17	0.00	0.04	6.36	0.01	0.10	36.98	8.70	0.00	0.37	0.02	48.46	101.04	0.78	0.16	0.15	0.91	3

Grains	Spots	SiO_2	MgO	MnO	CaO	ZnO	FeO	Al_2O_3	V_2O_3	Cr_2O_3	TiO_2	Total	SiO_2	MgO	MnO	CaO	ZnO	FeO	Fe_2O_3	Al_2O_3	V_2O_3	Cr_2O_3	TiO_2	Total	Ferrous Fe	Ferric Fe	Other cations	Ti	O
Fig. 5 (7)	1	0.00	0.05	0.45	0.00	0.03	79.16	0.00	0.39	0.05	11.50	91.63	0.00	0.05	0.45	0.00	0.03	9.78	77.08	0.00	0.39	0.05	11.50	99.33	0.22	1.53	0.03	0.23	3
	2	0.00	0.03	0.30	0.00	0.00	80.31	0.00	0.12	0.01	12.83	93.60	0.00	0.03	0.30	0.00	0.00	11.17	76.82	0.00	0.12	0.01	12.83	101.28	0.24	1.50	0.01	0.25	3
	3	0.00	0.00	0.36	0.01	0.07	77.86	0.00	0.40	0.08	13.78	92.56	0.00	0.00	0.36	0.01	0.07	11.95	73.22	0.00	0.40	0.08	13.78	99.87	0.26	1.45	0.03	0.27	3
	4	0.00	0.14	1.88	0.00	0.00	66.77	0.00	0.10	0.04	23.12	92.05	0.00	0.14	1.88	0.00	0.00	18.64	53.48	0.00	0.10	0.04	23.12	97.40	0.41	1.07	0.06	0.46	3
	5	0.00	0.17	1.85	0.02	0.00	66.19	0.00	0.20	0.06	23.84	92.33	0.00	0.17	1.85	0.02	0.00	19.26	52.14	0.00	0.20	0.06	23.84	97.54	0.43	1.04	0.07	0.48	3
	6	0.00	0.10	1.62	0.00	0.00	49.21	0.00	0.29	0.02	46.69	97.94	0.00	0.10	1.62	0.00	0.00	40.18	10.03	0.00	0.29	0.02	46.69	98.94	0.86	0.19	0.05	0.90	3
	7	0.00	0.12	1.50	0.01	0.02	49.51	0.00	0.28	0.02	47.06	98.52	0.00	0.12	1.50	0.01	0.02	40.58	9.92	0.00	0.28	0.02	47.06	99.51	0.86	0.19	0.04	0.90	3
	8	0.00	0.54	8.58	0.01	0.06	38.84	0.00	0.25	0.03	48.79	97.10	0.00	0.54	8.58	0.01	0.06	34.17	5.19	0.00	0.25	0.03	48.79	97.61	0.74	0.10	0.22	0.95	3
Fig. 5 (8)	1	0.00	0.09	0.04	0.02	0.00	78.46	0.13	0.68	0.10	12.41	91.92	0.00	0.09	0.04	0.02	0.00	10.95	75.00	0.13	0.68	0.10	12.41	99.41	0.24	1.49	0.03	0.25	3
	2	0.00	0.12	0.03	0.00	0.00	77.42	0.10	0.73	0.09	12.89	91.38	0.00	0.12	0.03	0.00	0.00	11.36	73.39	0.10	0.73	0.09	12.89	98.71	0.25	1.47	0.03	0.26	3
	3	0.00	0.70	0.37	0.00	0.08	50.94	0.01	0.39	0.03	45.14	97.64	0.00	0.70	0.37	0.00	0.08	38.92	13.35	0.01	0.39	0.03	45.14	98.97	0.83	0.26	0.05	0.87	3
	4	0.00	0.72	0.33	0.00	0.03	49.66	0.00	0.42	0.06	46.67	97.88	0.00	0.72	0.33	0.00	0.03	40.34	10.35	0.00	0.42	0.06	46.67	98.91	0.86	0.20	0.05	0.90	3
	5	0.00	0.74	0.34	0.01	0.00	48.66	0.00	0.40	0.01	47.35	97.51	0.00	0.74	0.34	0.01	0.00	40.91	8.60	0.00	0.40	0.01	47.35	98.37	0.88	0.17	0.05	0.91	3
Fig. 5 (9)	1	0.00	0.03	0.21	0.00	0.00	80.08	0.00	0.59	0.09	9.02	90.03	0.00	0.03	0.21	0.00	0.00	7.84	80.26	0.00	0.59	0.09	9.02	98.05	0.18	1.62	0.03	0.18	3
	2	0.00	0.03	0.14	0.01	0.00	79.79	0.00	0.61	0.05	9.81	90.44	0.00	0.03	0.14	0.01	0.00	8.61	79.08	0.00	0.61	0.05	9.81	98.34	0.19	1.59	0.03	0.20	3
	3	0.00	0.01	0.19	0.01	0.11	79.14	0.00	0.58	0.06	9.98	90.09	0.00	0.01	0.19	0.01	0.11	8.66	78.31	0.00	0.58	0.06	9.98	97.91	0.19	1.58	0.03	0.20	3
	4	0.00	0.05	0.19	0.00	0.00	78.47	0.00	0.51	0.08	11.84	91.14	0.00	0.05	0.19	0.00	0.00	10.37	75.66	0.00	0.51	0.08	11.84	98.70	0.23	1.51	0.03	0.24	3
	5	0.00	0.04	0.82	0.00	0.00	73.87	0.00	0.49	0.00	17.50	92.72	0.00	0.04	0.82	0.00	0.00	14.85	65.58	0.00	0.49	0.00	17.50	99.27	0.33	1.30	0.04	0.35	3
	10	0.00	0.18	1.65	0.02	0.00	51.63	0.00	0.39	0.05	42.63	96.55	0.00	0.18	1.65	0.02	0.00	36.33	17.00	0.00	0.39	0.05	42.63	98.25	0.79	0.33	0.06	0.83	3
	11	0.00	0.17	2.86	0.00	0.02	47.83	0.00	0.32	0.03	45.61	96.84	0.00	0.17	2.86	0.00	0.02	37.82	11.13	0.00	0.32	0.03	45.61	97.95	0.82	0.22	0.08	0.89	3
	12	0.00	0.22	1.86	0.00	0.02	48.59	0.00	0.43	0.03	46.78	97.93	0.00	0.22	1.86	0.00	0.02	39.78	9.79	0.00	0.43	0.03	46.78	98.91	0.85	0.19	0.06	0.90	3
	13	0.00	0.23	1.91	0.00	0.08	46.77	0.00	0.36	0.02	47.61	96.99	0.00	0.23	1.91	0.00	0.08	40.42	7.05	0.00	0.36	0.02	47.61	97.69	0.88	0.14	0.06	0.93	3
	14	0.00	0.19	1.94	0.01	0.10	46.57	0.00	0.40	0.00	48.60	97.81	0.00	0.19	1.94	0.01	0.10	41.32	5.83	0.00	0.40	0.00	48.60	98.39	0.89	0.11	0.06	0.94	3
	15	0.00	0.19	1.83	0.00	0.09	45.95	0.00	0.37	0.03	48.78	97.26	0.00	0.19	1.83	0.00	0.09	41.60	4.83	0.00	0.37	0.03	48.78	97.74	0.90	0.09	0.06	0.95	3
	16	0.00	0.17	1.97	0.00	0.14	45.70	0.00	0.41	0.00	49.38	97.77	0.00	0.17	1.97	0.00	0.14	42.00	4.11	0.00	0.41	0.00	49.38	98.17	0.90	0.08	0.06	0.96	3
	17	0.00	0.17	2.22	0.00	0.00	45.52	0.00	0.31	0.04	49.82	98.08	0.00	0.17	2.22	0.00	0.00	42.26	3.62	0.00	0.31	0.04	49.82	98.44	0.91	0.07	0.06	0.96	3

2) Partially Leucoxenated Ilmenite (4.6%)

Some of ilmenite grains showed patchy intergrowths of altered and unaltered ilmenite. It is likely that some of these grains were originally composed of subgraphic intergrowth of titanhematite and ferriilmenite as the major component. Patches of isotropic leucoxenated material formed along the periphery of the grain and are invading its inner part (Figure 6(3)). The zones of leucoxene invasion seem to have been relatively richer in the titanhematite component. The leucoxenated areas have dark brown colors under the reflected light. Between crossed nicols they have yellow and yellowish red internal reflections, most probably due to microcrystalline rutile. In other grains, a leucoxenated rim is completely surrounding the core of titanhematite-ferriilmenite subgraphic intergrowth (Figure 6(4)). The unaltered component of the grains is only ilmenite, containing parts of preexisting sphene and hence most of the leucoxenated areas seem to have initiated on ilmenite parts which were originally replaced by sphene (Figure 6(4)). We think that in case of partially leucoxenated grains, the unaltered component is prefered to be inhomogenous ilmenite. Furthermore, such partial leucoxenated zones have occured at low temperatures similar to those prevailing during weathering, transportation, deposition, and/or post-deposition processes affecting placer deposits. The majority of homogeneous ilmenite grains seem to be more stable and resistant to such partial leucoxenation. The process of ilmenite alteration into different varieties of leucoxene, passing with leached ilmenite, pseudorutile, leached pseudorutile, and even secondary rutile will be explained in another article, so it will not be not explained in detail here.

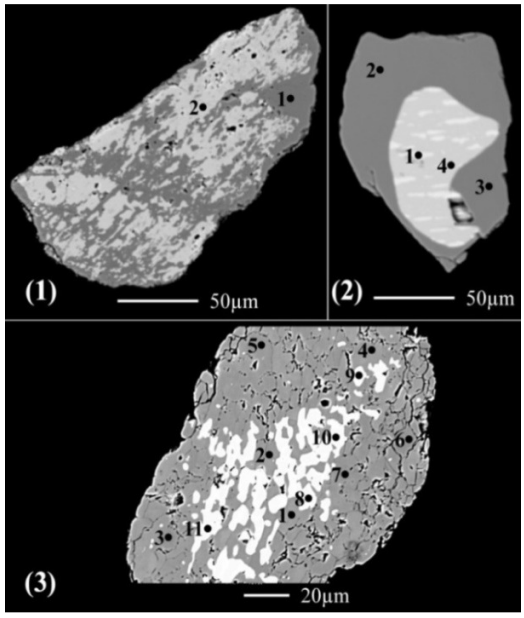

Fig. 7. BSE images of 3 different partially altered ilmenite grains into sphene.

3) Sphene-Ilmenite Intergrowth (1.2%)

Some ilmenite grains were detected to have altered and been replaced by sphene. Some grains were detected to be of fresh ilmenite cores completely surrounded by a sphene rim (Figure 7).

TABLE IV. CALCULATED MINERAL COMPONENT FRACTIONS INCLUDED WITHIN EACH MICROPROBE ANALYZED SPOT OF THE GRAINS OF FIGURES 4-5

Grains	Spots	SiO_2	MgO	MnO	CaO	ZnO	FeO	Fe_2O_3	Al_2O_3	V_2O_3	Cr_2O_3	TiO_2	Total	Method	Gek	Pyr	Ilm	H	R	Total
Fig. 4 (1)	1	3.09	2.30	0.40	0.12	0.07	34.59	8.28	0.59	0.54	0.04	39.59	89.62	M2	6.86	0.85	65.74	12.76	0.00	86.21
	2	3.46	2.20	0.35	0.70	0.22	35.90	5.13	0.82	0.60	0.02	41.27	90.66	M2	6.57	0.73	69.40	9.35	0.00	86.06
	3	1.82	2.34	0.43	0.16	0.07	34.85	6.71	0.92	0.60	0.00	41.74	89.63	M2	6.97	0.92	69.61	9.73	0.00	87.23
	4	3.69	2.73	0.44	0.08	0.08	38.26	1.81	1.33	0.58	0.02	43.73	92.75	M2	8.15	0.93	71.89	7.85	0.00	88.82
	5	0.12	2.33	0.33	0.02	0.02	38.01	5.00	0.06	0.51	0.06	47.13	93.58	M2	6.94	0.71	80.10	5.21	0.00	92.96
	6	0.17	2.42	0.40	0.02	0.03	38.09	6.87	0.10	0.55	0.03	47.43	96.12	M2	7.22	0.86	80.17	7.15	0.00	95.39
	7	0.00	2.57	0.43	0.03	0.13	37.57	8.96	0.06	0.56	0.00	47.51	97.82	M1	7.67	0.91	79.35	9.02	0.19	97.14
	8	0.00	2.54	0.41	0.02	0.09	37.98	8.21	0.04	0.62	0.03	47.82	97.75	M1	7.57	0.88	80.21	8.28	0.13	97.06
	9	0.00	2.52	0.38	0.05	0.06	38.07	8.82	0.09	0.55	0.00	47.88	98.41	M1	7.53	0.80	80.41	8.91	0.15	97.79
	10	0.15	2.11	0.38	0.02	0.00	39.07	3.06	0.05	0.54	0.02	47.89	93.28	M2	6.30	0.80	82.25	3.28	0.00	92.62
	11	0.00	2.52	0.47	0.00	0.07	38.10	8.53	0.08	0.60	0.01	47.95	98.34	M1	7.53	1.00	80.46	8.62	0.09	97.70
	12	0.10	2.25	0.37	0.05	0.03	39.54	3.03	0.07	0.56	0.00	48.78	94.77	M2	6.69	0.79	83.46	3.12	0.00	94.07
	13	0.16	2.01	0.36	0.06	0.04	40.78	1.07	0.07	0.58	0.02	49.63	94.78	M2	5.99	0.77	85.99	1.24	0.00	93.99
Fig. 4 (2)	1	0.02	1.26	0.51	0.00	0.42	14.18	60.21	3.15	1.25	1.17	19.22	101.40	M1	3.74	1.09	29.95	64.53	0.40	99.72
	2	0.02	1.51	0.44	0.03	0.35	16.69	55.47	2.99	1.18	1.06	22.40	102.13	M1	4.51	0.94	35.25	59.51	0.37	100.58
	3	0.12	4.61	0.49	0.06	0.00	34.83	8.27	0.08	0.51	0.08	48.32	97.35	M2	13.74	1.04	73.48	8.46	0.00	96.72
	4	0.20	4.26	0.54	0.09	0.08	35.69	8.54	0.12	0.49	0.10	48.66	98.76	M2	12.71	1.14	75.31	8.80	0.00	97.97
	5	0.00	3.66	0.56	0.03	0.06	38.11	7.20	0.13	0.50	0.11	50.34	100.71	M1	10.92	1.19	80.49	7.45	0.12	100.17
	6	0.00	3.59	0.61	0.02	0.08	38.26	6.47	0.11	0.58	0.15	50.45	100.32	M1	10.71	1.29	80.81	6.73	0.13	99.69
	7	0.00	3.54	0.62	0.03	0.01	39.11	6.09	0.14	0.51	0.15	51.24	101.42	M1	10.56	1.31	82.60	6.37	0.07	100.92
	8	0.00	3.74	0.55	0.01	0.00	38.96	6.42	0.09	0.56	0.13	51.34	101.79	M1	11.14	1.17	82.27	6.65	0.04	101.27
Fig. 4 (3)	1	0.00	0.08	0.71	0.00	0.00	16.34	66.95	0.00	0.47	0.06	19.12	103.73	M1	0.22	1.52	34.51	67.01	0.00	103.26
	2	0.00	0.08	0.71	0.00	0.00	17.99	63.79	0.00	0.44	0.07	20.94	104.01	M1	0.23	1.50	37.99	63.86	0.00	103.58
	3	0.00	0.08	1.12	0.00	0.04	26.46	43.53	0.00	0.45	0.04	30.88	102.60	M1	0.23	2.39	55.89	43.57	0.05	102.13
	4	0.00	0.12	1.89	0.01	0.00	44.56	0.51	0.00	0.35	0.00	51.92	99.36	M1	0.35	4.01	94.12	0.51	0.02	99.02
	5	0.00	0.13	1.66	0.00	0.02	45.01	0.54	0.00	0.32	0.00	52.17	99.85	M1	0.38	3.53	95.05	0.54	0.02	99.53
	6	0.00	0.17	1.86	0.01	0.10	44.69	0.08	0.00	0.42	0.01	52.20	99.52	M1	0.50	3.95	94.39	0.09	0.11	99.03
	7	0.00	0.15	1.85	0.03	0.00	44.81	0.45	0.00	0.39	0.00	52.24	99.92	M1	0.44	3.94	94.64	0.45	0.05	99.52
	8	0.00	0.11	1.73	0.00	0.00	45.18	0.02	0.00	0.37	0.01	52.40	99.84	M1	0.34	3.68	95.43	0.03	0.00	99.49
Fig. 4 (4)	1	0.00	0.05	0.32	0.00	0.00	8.82	77.72	0.00	0.39	0.12	10.26	97.68	M1	0.14	0.68	18.63	77.84	0.01	97.29
	2	0.00	0.04	0.36	0.02	0.00	9.09	76.65	0.00	0.39	0.08	10.62	97.25	M1	0.10	0.77	19.21	76.73	0.03	96.84
	3	0.00	0.06	0.54	0.01	0.00	11.10	72.00	0.00	0.36	0.10	13.07	97.24	M1	0.16	1.14	23.45	72.11	0.01	96.88
	4	0.00	0.05	0.85	0.02	0.02	13.71	66.06	0.00	0.35	0.08	16.34	97.47	M1	0.14	1.81	28.95	66.13	0.05	97.08
	5	0.88	0.23	3.42	0.07	0.05	39.20	0.00	0.00	0.33	0.02	49.60	93.48	M1	0.69	7.28	82.79	0.02	1.72	92.50
	6	0.00	0.28	3.50	0.00	0.00	41.10	2.36	0.00	0.34	0.00	50.18	97.76	M1	0.83	7.43	86.80	2.37	0.01	97.45
	7	0.00	0.33	3.57	0.02	0.02	41.23	1.77	0.00	0.34	0.03	50.53	97.83	M1	0.97	7.59	87.07	1.80	0.04	97.48
	8	0.00	0.35	3.58	0.04	0.21	40.98	2.01	0.00	0.32	0.01	50.54	98.03	M1	1.04	7.62	86.55	2.02	0.26	97.49
	9	0.00	0.32	3.66	0.00	0.06	41.16	2.17	0.00	0.28	0.01	50.57	98.23	M1	0.96	7.79	86.92	2.18	0.06	97.91
	10	0.00	0.24	3.69	0.00	0.00	41.97	0.47	0.00	0.33	0.07	51.29	98.07	M1	0.73	7.85	88.63	0.54	0.01	97.76
Fig. 4 (5)	1	0.00	0.01	0.44	0.00	0.01	10.97	72.99	0.00	0.66	0.51	12.71	98.30	M1	0.02	0.92	23.17	73.50	0.01	97.63
	2	0.00	0.05	0.49	0.01	0.14	10.72	72.86	0.00	0.56	0.44	12.73	98.00	M1	0.15	1.05	22.64	73.30	0.15	97.30
	3	0.00	0.01	0.22	0.03	0.00	17.35	57.53	0.00	0.69	0.47	19.58	95.87	M1	0.01	0.47	36.64	58.00	0.04	95.17
	4	0.00	0.00	0.06	0.03	0.00	28.69	34.36	0.00	0.63	0.48	32.00	96.25	M1	0.00	0.13	60.59	34.83	0.05	95.59
	5	0.03	0.05	0.15	0.06	0.05	29.98	0.00	0.00	0.67	0.29	65.39	96.68	M3	0.15	0.32	0.00	33.61	65.12	99.20
	6	0.00	0.06	0.18	0.03	0.04	20.14	0.00	0.00	0.60	0.11	72.53	93.69	M3	0.19	0.39	0.00	22.49	72.20	95.27
	7	0.00	0.02	0.15	0.01	0.00	18.16	0.00	0.00	0.69	0.14	74.65	93.82	M3	0.04	0.32	0.00	20.32	74.45	95.14
	8	0.02	0.02	0.19	0.02	0.00	18.20	0.00	0.00	0.60	0.02	76.26	95.32	M3	0.05	0.40	0.00	20.25	76.01	96.71
	9	0.00	0.04	0.09	0.01	0.00	5.37	0.00	0.00	0.87	0.09	93.43	99.89	M3	0.11	0.18	0.00	6.05	93.27	99.61
	10	0.09	0.00	0.91	0.11	0.00	40.02	6.15	0.00	0.40	0.08	45.55	93.29	M1	0.00	1.93	84.51	6.22	0.04	92.71
	11	0.05	0.11	6.22	0.06	0.11	35.04	9.73	0.00	0.34	0.08	46.29	98.02	M1	0.33	13.21	74.01	9.81	0.13	97.49
	12	0.00	0.48	3.50	0.11	0.03	38.28	7.92	0.00	0.34	0.05	47.63	98.34	M1	1.43	7.44	80.86	7.97	0.19	97.89
	13	0.00	0.47	4.19	0.00	0.08	38.27	6.49	0.00	0.41	0.05	48.27	98.23	M1	1.40	8.90	80.83	6.54	0.09	97.76
	14	0.00	0.07	0.35	0.01	0.00	41.90	0.00	0.00	0.47	0.11	48.99	91.67	M1	0.20	0.74	88.49	0.11	1.89	91.44
	15	0.02	0.34	2.20	0.05	0.03	38.30	0.00	0.00	0.46	0.16	51.28	92.33	M1	1.00	4.67	80.89	0.16	5.57	92.29
Fig. 4 (6)	1	0.00	0.00	0.02	0.01	0.03	5.18	94.61	0.00	0.15	0.03	5.81	105.83	M1	0.01	0.04	10.93	94.64	0.04	105.65
	2	0.03	0.00	0.26	0.01	0.06	6.81	87.84	0.00	0.13	0.07	7.90	103.10	M1	0.01	0.54	14.38	87.90	0.04	102.88
	3	0.00	0.03	0.42	0.01	0.03	11.17	76.69	0.00	0.39	0.06	12.99	101.78	M1	0.08	0.89	23.60	76.74	0.05	101.36
	4	0.00	0.03	0.57	0.00	0.00	11.65	74.89	0.00	0.43	0.12	13.66	101.34	M1	0.10	1.21	24.61	75.01	0.00	100.92
	5	0.00	0.01	0.66	0.00	0.07	11.57	75.60	0.00	0.49	0.10	13.69	102.19	M1	0.04	1.40	24.43	75.70	0.07	101.64
	6	3.31	0.17	0.34	0.12	0.07	39.19	5.37	0.02	0.45	0.10	40.11	89.26	M2	0.50	0.72	74.86	9.66	0.00	85.74
	7	0.04	0.09	6.64	0.09	0.01	35.61	7.93	0.00	0.33	0.01	47.33	98.07	M1	0.27	14.11	75.21	7.94	0.10	97.63

Grains	Spots	SiO_2	MgO	MnO	CaO	ZnO	FeO	Fe_2O_3	Al_2O_3	V_2O_3	Cr_2O_3	TiO_2	Total	Method	Gek	Pyr	Ilm	H	R	Total
Fig. 4 (6)	8	0.00	0.04	6.36	0.01	0.10	36.98	8.70	0.00	0.37	0.02	48.46	101.04	M1	0.11	13.53	78.10	8.72	0.12	100.58
	9	0.00	0.00	0.31	0.03	0.00	37.02	0.00	0.00	0.43	0.02	57.60	95.40	M3	0.01	0.65	0.00	41.16	57.25	99.06
	10	0.00	0.03	0.14	0.02	0.01	22.82	0.00	0.00	0.56	0.04	74.81	98.42	M3	0.08	0.29	0.00	25.41	74.60	100.38
	11	0.00	0.02	0.03	0.00	0.05	12.45	0.00	0.00	0.64	0.01	86.25	99.45	M3	0.07	0.06	0.00	13.85	86.17	100.15
	12	0.00	0.00	0.00	0.01	0.00	5.84	0.00	0.00	0.64	0.00	93.48	99.97	M3	0.00	0.00	0.00	6.49	93.48	99.97
	13	0.07	0.00	0.02	0.03	0.00	4.37	0.00	0.00	0.67	0.01	93.87	99.04	M3	0.00	0.03	0.00	4.87	93.86	98.76
Fig. 5 (7)	1	0.00	0.05	0.45	0.00	0.03	9.78	77.08	0.00	0.39	0.05	11.50	99.33	M1	0.16	0.95	20.66	77.13	0.03	98.92
	2	0.00	0.03	0.30	0.00	0.00	11.17	76.82	0.00	0.12	0.01	12.83	101.28	M1	0.10	0.64	23.59	76.82	0.01	101.16
	3	0.00	0.00	0.36	0.01	0.07	11.95	73.22	0.00	0.40	0.08	13.78	99.87	M1	0.00	0.77	25.24	73.30	0.09	99.40
	4	0.00	0.14	1.88	0.00	0.00	18.64	53.48	0.00	0.10	0.04	23.12	97.40	M1	0.43	4.00	39.36	53.52	0.00	97.31
	5	0.00	0.17	1.85	0.02	0.00	19.26	52.14	0.00	0.20	0.06	23.84	97.54	M1	0.50	3.93	40.68	52.20	0.03	97.33
	6	0.00	0.10	1.62	0.00	0.00	40.18	10.03	0.00	0.29	0.02	46.69	98.94	M1	0.29	3.44	84.87	10.05	0.01	98.66
	7	0.00	0.12	1.50	0.01	0.02	40.58	9.92	0.00	0.28	0.02	47.06	99.51	M1	0.35	3.20	85.70	9.94	0.03	99.22
	8	0.00	0.54	8.58	0.01	0.06	34.17	5.19	0.00	0.25	0.03	48.79	97.61	M1	1.62	18.23	72.17	5.22	0.08	97.33
	9	0.00	0.06	0.14	0.00	0.07	32.64	0.00	0.00	0.37	0.00	59.82	93.10	M3	0.18	0.30	0.00	36.27	59.54	96.29
	10	9.17	0.52	0.51	0.21	0.08	10.16	0.00	1.36	0.43	0.00	69.65	92.10	M3	1.54	1.09	0.00	12.65	68.06	83.34
Fig. 5 (8)	1	0.00	0.09	0.04	0.02	0.00	10.95	75.00	0.13	0.68	0.10	12.41	99.41	M1	0.25	0.09	23.12	75.24	0.03	98.72
	2	0.00	0.12	0.03	0.00	0.00	11.36	73.39	0.10	0.73	0.09	12.89	98.71	M1	0.35	0.06	23.99	73.59	0.00	97.99
	3	0.00	0.70	0.37	0.00	0.08	38.92	13.35	0.01	0.39	0.03	45.14	98.97	M1	2.07	0.78	82.21	13.38	0.08	98.53
	4	0.00	0.72	0.33	0.00	0.03	40.34	10.35	0.00	0.42	0.06	46.67	98.91	M1	2.15	0.70	85.20	10.41	0.03	98.49
	5	0.00	0.74	0.34	0.01	0.00	40.91	8.60	0.00	0.40	0.01	47.35	98.37	M1	2.22	0.72	86.41	8.62	0.02	97.98
Fig. 5 (9)	1	0.00	0.03	0.21	0.00	0.00	7.84	80.26	0.00	0.59	0.09	9.02	98.05	M1	0.10	0.44	16.56	80.36	0.01	97.46
	2	0.00	0.03	0.14	0.01	0.00	8.61	79.08	0.00	0.61	0.05	9.81	98.34	M1	0.10	0.30	18.18	79.13	0.02	97.72
	3	0.00	0.01	0.19	0.01	0.11	8.66	78.31	0.00	0.58	0.06	9.98	97.91	M1	0.02	0.40	18.29	78.36	0.13	97.20
	4	0.00	0.05	0.19	0.00	0.00	10.37	75.66	0.00	0.51	0.08	11.84	98.70	M1	0.15	0.41	21.90	75.74	0.00	98.20
	5	0.00	0.04	0.82	0.00	0.00	14.85	65.58	0.00	0.49	0.00	17.50	99.27	M1	0.10	1.74	31.36	65.58	0.00	98.78
	6	0.00	0.23	0.17	0.02	0.00	32.80	0.00	0.00	0.45	0.06	57.45	91.18							
	7	0.00	0.21	0.42	0.02	0.06	31.86	0.00	0.00	0.43	0.02	58.55	91.58							
	8	0.00	0.34	0.18	0.03	0.02	21.06	0.00	0.00	0.52	0.01	71.88	94.03							
	9	0.00	0.26	0.16	0.00	0.00	12.39	0.00	0.00	0.62	0.01	82.73	96.16							
	10	0.00	0.18	1.65	0.02	0.00	36.33	17.00	0.00	0.39	0.05	42.63	98.25	M1	0.53	3.50	76.73	17.06	0.03	97.86
	11	0.00	0.17	2.86	0.00	0.02	37.82	11.13	0.00	0.32	0.03	45.61	97.95	M1	0.50	6.07	79.87	11.15	0.03	97.63
	12	0.00	0.22	1.86	0.00	0.02	39.78	9.79	0.00	0.43	0.03	46.78	98.91	M1	0.65	3.96	84.02	9.82	0.02	98.48
	13	0.00	0.23	1.91	0.00	0.08	40.42	7.05	0.00	0.36	0.02	47.61	97.69	M1	0.68	4.05	85.37	7.08	0.09	97.27
	14	0.00	0.19	1.94	0.01	0.10	41.32	5.83	0.00	0.40	0.00	48.60	98.39	M1	0.55	4.13	87.27	5.83	0.11	97.90
	15	0.00	0.19	1.83	0.00	0.09	41.60	4.83	0.00	0.37	0.03	48.78	97.74	M1	0.57	3.90	87.86	4.86	0.10	97.29
	16	0.00	0.17	1.97	0.00	0.14	42.00	4.11	0.00	0.41	0.00	49.38	98.17	M1	0.50	4.19	88.70	4.11	0.14	97.65
	17	0.00	0.17	2.22	0.00	0.00	42.26	3.62	0.00	0.31	0.04	49.82	98.44	M1	0.52	4.71	89.26	3.66	0.01	98.15

TABLE V. MICROPROBE CHEMICAL ANALYSIS OF THE SPOTS OF SOME DETECTED PARTIALLY ALTERED ILMENITE GRAINS OF FIGURE 7. THE CALCULATED MOLECULAR FORMULAE ARE GIVEN FOR THE SPOTS COMPOSED ESSENTIALLY OF ILMENITE; SPOT 2 OF (1), SPOTS 1, 4 OF (2) AND SPOTS 8-10 OF (3). SPOT 11 OF (3) IS LEACHED ILMENITE WHILE THE OTHER REMAINING SPOTS ARE SPHENE

Grains	Spots	SiO_2	MgO	MnO	CaO	ZnO	FeO	Al_2O_3	V_2O_3	Cr_2O_3	TiO_2	Total	SiO_2	MgO	MnO	CaO	Zn	FeO	Fe_2O_3	Al_2O_3	V_2O_3	Cr_2O_3	TiO_2	Total	Ferrous Fe	Ferric Fe	Other cations	Ti	O
Fig. 7 (1)	1	30.67	0.00	0.12	28.50	0.01	1.26	0.85	0.39	0.00	37.67	99.48																	
	2	0.00	0.06	2.00	0.25	0.00	44.42	0.00	0.58	0.00	51.29	98.61	0.00	0.06	2.00	0.25	0.00	43.68	0.82	0.00	0.58	0.00	51.29	98.69	0.93	0.02	0.06	0.99	3
Fig. 7 (2)	1	0.00	0.01	0.15	0.05	0.00	81.87	0.00	0.53	0.06	8.34	91.01	0.00	0.01	0.15	0.05	0.00	7.26	82.89	0.00	0.53	0.06	8.34	99.28	0.16	1.65	0.02	0.17	3
	2	30.73	0.00	0.08	28.58	0.00	0.63	1.01	0.31	0.00	38.03	99.38																	
	3	30.76	0.00	0.15	28.82	0.00	0.99	0.93	0.26	0.04	38.29	100.24																	
	4	0.00	0.20	3.40	0.17	0.00	43.94	0.00	0.43	0.00	50.48	98.63	0.00	0.20	3.40	0.17	0.00	41.39	2.84	0.00	0.43	0.00	50.48	98.91	0.88	0.05	0.10	0.97	3
Fig. 7 (3)	1	30.11	0.00	0.07	28.41		0.98	0.83		0.23	38.77	99.41																	
	2	30.26	0.00	0.04	28.08		0.94	0.22		0.47	39.33	99.32																	
	3	30.38	0.00	0.00	28.50		0.28	0.62		0.16	39.71	99.65																	
	4	30.46	0.00	0.00	28.75		0.41	0.54		0.13	39.91	100.21																	
	5	30.15	0.00	0.01	28.54		0.54	0.56		0.23	39.93	99.96																	
	6	30.19	0.03	0.00	28.60		0.26	0.46		0.10	40.06	99.70																	
	7	30.28	0.00	0.04	28.74		0.26	0.76		0.09	40.10	100.27																	
	8	0.35	0.17	8.68	0.80		34.89	0.00		0.05	53.10	98.04	0.35	0.17	8.68	0.80	0.00	38.78	0.00	0.00	0.00	0.05	53.10	97.68	0.84	0.00	0.22	1.02	3
	9	0.05	0.19	11.19	1.07		34.40	0.00		0.02	53.34	100.26	0.05	0.19	11.19	1.07	0.00	38.23	0.00	0.00	0.00	0.02	53.34	100.19	0.72	0.00	0.27	1.00	3
	10	0.02	0.20	10.13	0.74		35.72	0.00		0.04	53.54	100.39	0.02	0.20	10.13	0.74	0.00	39.67	0.00	0.00	0.00	0.04	53.54	100.29	0.74	0.00	0.24	1.01	3
	11	0.05	0.19	5.71	0.76		30.88	0.00		0.05	58.44	96.07																	

Furthermore, some grains were found to be partially replaced by sphene where half of the grain is fresh ilmenite and the rest is replaced by sphene. The complete absence of cavities or cracks between ilmenite and sphene indicates that the replacement process took place volume by volume [12]. According to [23], sphene is developed by magmatic resorption or hydrothermal action. Under the reflected light, the sphene is light grey with a reflectivity much lower than that of ilmenite, but somewhat higher than that of the gangue silicate minerals. In fact, its reflectivity is somewhat similar to that of cassiterite or zircon. Under crossed nicols, sphene exhibits an obvious anisotropism. However, its abundant white or slightly greyish white internal reflections may mask it.

Some of the grains composed of ilmenite associated with sphene are detected in Figure 7 (1)-(3). Spots 1 in grain (1), 2-3 in grain (2), and 1-7 in grain (3) are sphene substituting ilmenite (Figure 7, Table V). Spot 11 in grain (3) is leached ilmenite having the chemical composition of Fe^{2+} (0.12%), Fe^{3+} (1.64%), other cations (0.41%), Ti_3, and O_9. The losed iron cations are equal to 0.82 and the sum of total oxides is 99.28%. Spot 2 of grain (1) consists of 92.29% ilmenite, 4.25% pyrophanite, 0.80% hematite, 0.30% geikielite, and 0.38% rutile. Spots 1, 4 of grain (2) (Figure 7), are titanhematite-ferriilmenite exsolved intergrowths surrounded by sphene (spots 2-3). Spot 1 is titanhematite having MnO content similar to spot 3 of the sphene. In spot 1, it is obvious that V^{3+} follows Fe^{3+} rather than Fe^{2+}, while Mn^{2+} follows Fe^{2+} rather than Fe^{3+}. The spot is composed of 83% hematite, 15.42% ilmenite, 0.43% pyrophanite, and 0.04% rutile. Spot 4 is ferriilmenite with a relatively higher MnO content (3.4%). The spot consists of 87.44% ilmenite, 7.23% pyrophanite, 2.8% hematite, 0.6% geikielite, and 0.27% rutile.

Spots 8-10 in grain (3) seem to be ilmenite with relatively higher MnO content (Table V). This grain may indicate that both FeO and MnO are replaced by SiO_2 and CaO while the TiO_2 content remains stable to form sphene replacing ilmenite. The comparison of MnO content of spot 11 with the MnO content of spots 8-10 reflects that MnO is lost during the early stages of ilmenite alteration during the leaching of Fe^{3+}. Also, it is detected that the Cr_2O_3 content is relatively much higher in the sphene spots than in ilmenite spots which ensures that Cr_2O_3 does not follow TiO_2 content. These 3 last grains reflect the association of some ilmenite grains within the obtained final ilmenite concentrate with the sphene which may responsible for the increment of the SiO_2 and CaO content of the concentrate. Also, the ilmenite component associated to or replaced by sphene is characteristic with a relatively higher content of pyrophanite and hence MnO.

VI. CONCLUSION

The obtained Egyptian beach ilmenite concentrate from east Rosetta area contains several mineral textures. The homogeneous ilmenite represents 63wt% of the detected ilmenite varieties. Some of the homogeneous ilmenite grains are characterized by more MgO than MnO content, while the opposite occurs in the other grains. The reason for this is the presence of geikielite and pyrophanite solid solutions in different contents. In the homogeneous ilmenite grains the contents of MgO and MnO range between 0.0 and 3.1wt% and 0.4 and 6.1wt% respectively. Some of the detected homogeneous ferriilmenite grains are associated with the bulk ilmenite grains (2wt%). The included dissolved Fe_2O_3 ranges between 7.3 and 22.8wt%. Their MgO, Al_2O_3, and Cr_2O_3 contents are relatively higher. The detected hematite-ilmenite exsolved intergrowth represents 21.4wt%, and may show 1 or 2 distinct generations of exsolutions.

Some minor composite grains are detected in the concentrate under examination. Each of them consists of two parts, one of them is titanhematite-ferriilmenite and the other ferriilmenite-titanhematite. The Fe_2O_3 contents of the ferriilmenite exsolved intergrowth of the different hematite-ilmenite grains varies and ranges between 0.02 and 17wt%. In some ferriilmenite components, the MnO ranges between 1.5 and 8.6wt%. In the composite ilmenite-hematite grains, the content of both MnO and MgO is relatively lower and can be also distributed homogeneously through the analyzed spots.

In the titanhematite components, the TiO_2 content ranges between 5.8 and 23.8wt%. The TiO_2 content rarely attains relatively greater value, 30.88wt%, where an individual amount of TiO_2 is postulated to occur with the ilmenite component within the titanhematite. The content of the associated MnO is relatively lower, i.e. 0.3-1.9wt%, in comparison with those of the ferriilmenite bodies. It is very low in the titanhematite of the detected composite grains. The solubility of MnO with ilmenite seems to be a relatively greater than with hematite. Both MgO and MnO are positively correlated with FeO rather than Fe_2O_3. It was also detected that V_2O_3 follows TiO_2 in spots of ferriilmenite and Fe_2O_3 rather than TiO_2 or FeO in spots of titanhematite.

In the investigated hematite-ilmenite exsolved intergrowthed grains, the Cr_2O_3 and Al_2O_3 contents of all the analyzed spots for the 2 exsolved components range between 0 and 1.2wt% and 0 and 3.2wt% respectively. Relatively greater content is present in the titanhematite components. In some titanhematite components, it was detected that the mechanism of leaching Fe_2O_3 is associated with the presence of molecular water which seems to be recycled and the associated SiO_2 and/or Al_2O_3 are enriched and finally precipitated inside spots and cracks. Generally, it was noticed that the presence of molecular water is important in the alteration process of ilmenite or some associated silicate mineral impurities. The partially altered ilmenite grains represent 7.34wt% and contain a relatively higher MnO content in their ilmenite components. The presence of sphene in the obtained ilmenite concentrate may be responsible for the recorded amounts of SiO_2 and CaO and maybe for some of the recorded Cr_2O_3 content.

As a final conclusion it is obvious that a considerable number of ilmenite grains contained in the final obtained high-purity ilmenite concentrate (more than 99wt% ilmenite) have exsolved intergrowthed components containing relatively higher quantities of Fe_2O_3, Cr_2O_3, SiO_2, and CaO. These intergrowths may be responsible for the relatively higher values of the recorded impurity oxides and hence the relatively lower TiO_2 and higher Fe_2O_3 and Cr_2O_3 content, for most of the obtained Egyptian beach ilmenite concentrates. Magnetic separation treatment, grain size differentiation, or both, of the

obtained ilmenite concentrate may improve the marketable specifications of the obtained ilmenite concentrate.

ACKNOWLEDGEMENT

The author wishes to express his appreciation to the Deputyship for Research & Innovation, Ministry of Education, Saudi Arabia for funding this research work.

REFERENCES

[1] E. M. El Shazly, "Classification of Egyptian Mineral Deposits," *Egyptian Journal of Geology*, vol. 1, no. 1, pp. 1–20, 1957.

[2] M. I. Moustafa, "Mineralogy and beneficiation of some economic minerals in the Egyptian black sands," Ph.D. dissertation, Mansoura University, Mansoura, Egypt, 1999.

[3] M. I. Moustafa, "Separation of economic minerals and discovery of zinc, lead and mercury minerals in the Egyptian black sands," in *The Third International Conference of the Geology of Africa*, Assiut, Egypt, 2003, pp. 153–171.

[4] M. I. Moustafa, "Separation of economic minerals and discovery of zinc, lead and mercury minerals in the Egyptian black sands," in *The Fifth International Conference of the Geology of Africa*, Assiut, Egypt, 2007, pp. 63–78.

[5] A. A. Mahessar *et al.*, "Sediment Transport Dynamics in the Upper Nara Canal Off-taking from Sukkur Barrage of Indus River," *Engineering, Technology & Applied Science Research*, vol. 10, no. 6, pp. 6563–6569, Dec. 2020, https://doi.org/10.48084/etasr.3924.

[6] N. P.H. Padmanabhan, T. Sreenivas, and N. K. Rao, "Processing of Ores of Titanium, Zirconium, Hafnium, Niobium, Tantalum, Molybdenum, Rhenium, and Tungsten: International Trends and the Indian Scene," *High Temperature Materials and Processes*, vol. 9, no. 2–4, pp. 217–248, Jul. 1990, https://doi.org/10.1515/HTMP.1990.9.2-4.217.

[7] R. X. Sinha, *Industrial minerals*. Oxford, UK: Metal Bulletin Books, 1982.

[8] E. E. El-Hinnawi, "Mineralogical and geochemical studies on Egyptian (U.A.R.) black sands," *Beitrage zur Mineralogie und Petrographie*, vol. 9, no. 6, pp. 519–532, Nov. 1964, https://doi.org/10.1007/BF01104489.

[9] N. Z. Boctor, "Mineralogical study of the opaque minerals in Rosetta-Damietta black sands," M.S. thesis, Cairo University, Giza, Egypt, 1966.

[10] N. M. Hammoud, "Concentration of monazite from Egyptian black sands, employing industrial techniques," M.S. thesis, Cairo University, Giza, Egypt, 1966.

[11] N. M. S. Hammoud, "A process for recovery of low chromium high grade ilmenite from north Egyptian beach deposits," in *Proceedings, 11th Indust. Mineral Process Conference*, Sardegna, Italy, 1975.

[12] M. A. Mikhail, "Distribution and sedimentation of ilmenite in black sands, west of Rosetta," M.S. thesis, Cairo University, Cairo, Egypt, 1971.

[13] A. A. Dewedar, "Comparative studies on the heavy minerals in some black sands deposits from Sinai and east Rosetta with contribution to the mineralogy and economics of their garnets," Ph.D. dissertation, El Menoufia University, Shebin El Koum, Egypt, 1997.

[14] A. A. El-Kammar, A. A. Ragab, and M. I. Moustafa, "Geochemistry of economic heavy minerals from Rosetta black sand of Egypt," *Journal of King Abdulaziz University: Earth Sciences*, vol. 22, no. 2, pp. 69–97, 2011, https://doi.org/10.4197/Ear.22-2.4.

[15] A.-A. M. Abdel-Karim, S. M. Zaid, M. I. Moustafa, and M. G. Barakat, "Mineralogy, chemistry and radioactivity of the heavy minerals in the black sands, along the northern coast of Egypt," *Journal of African Earth Sciences*, vol. 123, pp. 10–20, Nov. 2016, https://doi.org/10.1016/j.jafrearsci.2016.07.005.

[16] A.-A. M. Abdel-Karim, M. I. Moustafa, A. H. El-Afandy, and M. G. Barakat, "Mineralogy, Chemical Characteristics and Upgrading of Beach Ilmenite of the Top Meter of Black Sand Deposits of the Kafr Al-Sheikh Governorate, Northern Egypt," *Acta Geologica Sinica - English Edition*, vol. 91, no. 4, pp. 1326–1338, 2017, https://doi.org/10.1111/1755-6724.13364.

[17] M. A. M. Mahmoud, "The Environmental and Radiological Impacts in Abu Ghalaga Ilmenite Mine, South Eastern Desert, Egypt," *International Journal of Mining Science*, vol. 7, no. 1, pp. 10–19, 2021, https://doi.org/10.20431/2454-9460.0701002.

[18] A. M. Ramadan, M. Farghaly, W. M. Fathy, and M. M. Ahmed, "Leaching and kinetics studies on processing of Abu-Ghalaga ilmenite ore," *International Research Journal of Engineering and Technology*, vol. 3, no. 10, pp. 46–53, 2016.

[19] H. Awad *et al.*, "Mineralogy and Radioactivity Level of the New Occurrence of Ilmenite Bearing Gabbro at Abu Murrat, Northeastern Desert, Egypt," *Romanian Journal of Physics*, vol. 67, Mar. 2022, Art. no. 803.

[20] M. I. Moustafa, M. A. Tashkandi, and A. M. El-Sherif, "Detecting Mineral Resources and Suggesting a Physical Concentration Flowsheet for Economic Minerals at the Northern Border Region of Saudi Arabia," *Engineering, Technology & Applied Science Research*, vol. 12, no. 3, pp. 8617–8627, Jun. 2022, https://doi.org/10.48084/etasr.4894.

[21] G. T. R. Droop, "A general equation for estimating Fe3+ concentrations in ferromagnesian silicates and oxides from microprobe analyses, using stoichiometric criteria," *Mineralogical Magazine*, vol. 51, no. 361, pp. 431–435, Sep. 1987, https://doi.org/10.1180/minmag.1987.051.361.10.

[22] W. Uytenbogaardt and E. A. J. Burke, *Tables for Microscopic Identification of Ore Minerals*. Amsterdam, Netherlands: Elsevier, 1971.

[23] V. P. Ramadohr, "Die beziehungen von Fe-Ti-erzen aus magmatischen gesteinen," *Bulletin De La Commission Geologique De Finlande*, no. 173, pp. 1–18, 1956.

[24] J. R. Balsley and A. F. Buddington, "Iron-titanium oxide minerals, rocks, and aeromagnetic anomalies of the Adirondack area, New York," *Economic Geology*, vol. 53, no. 7, pp. 777–805, Nov. 1958, https://doi.org/10.2113/gsecongeo.53.7.777.

[25] D. I. Groves, S. E. Ho, N. M. S. Rock, M. E. Barley, and M. T. Muggeridge, "Archean cratons, diamond and platinum: Evidence for coupled long-lived crust-mantle systems," *Geology*, vol. 15, no. 9, pp. 801–805, Sep. 1987, https://doi.org/10.1130/0091-7613(1987)15<801:ACDAPE>2.0.CO;2.

[26] S. J. Barnes and V. Y. Kunilov, "Spinels and Mg Ilmenites from the Noril'sk 1 and Talnakh Intrusions and Other Mafic Rocks of the Siberian Flood Basalt Province," *Economic Geology*, vol. 95, no. 8, pp. 1701–1717, Dec. 2000, https://doi.org/10.2113/gsecongeo.95.8.1701.

[27] M. I. Pownceby, "Alteration and associated impurity element enrichment in detrital ilmenites from the Murray Basin, southeast Australia: a product of multistage alteration," *Australian Journal of Earth Sciences*, vol. 57, no. 2, pp. 243–258, Mar. 2010, https://doi.org/10.1080/08120090903521705.

[28] G. Pe-Piper, D. J. W. Piper, and L. Dolansky, "Alteration of Ilmenite in the Cretaceous Sandstones of Nova Scotia, Southeastern Canada," *Clays and Clay Minerals*, vol. 53, no. 5, pp. 490–510, Oct. 2005, https://doi.org/10.1346/CCMN.2005.0530506.

[29] D. P. Svisero and N. Z. Boctor, "Iron-titanium oxide and sulfide minerals in carbonatite from Jacupiranga, Brazil," *Annual report of the director of the geophysical laboratory*, vol. 77, pp. 876–880, 1978.

[30] R. H. Mitchell, "Manganoan magnesian ilmenite and titanian clinohumite from the Jacupiranga carbonatite, Sao Paulo, Brazil," *American Mineralogist*, vol. 63, no. 5–6, pp. 544–547, Jun. 1978.

[31] D. S. Rao and D. Sengupta, "Electron Microscopic Studies of Ilmenite from the Chhatrapur Coast, Odisha, India, and Their Implications in Processing," *Journal of Geochemistry*, vol. 2014, Jul. 2014, Art. no. e192639, https://doi.org/10.1155/2014/192639.

[32] J. C. Gaspar and P. J. Wyllie, "Ilmenite (high Mg,Mn,Nb) in the carbonatites from the Jacupiranga Complex, Brazil," *American Mineralogist*, vol. 68, no. 9–10, pp. 960–971, Oct. 1983.

[33] E. M. Khairy, M. K. Hussien, F. M. Nakhla, and S. S. Tawil, "Analysis and composition of Egyptian ilmenite ores from Abu Ghalaga and Rosetta,"*Journal of Geology*, *United Arab Republic*, vol. 8, no. 1, pp. 1-9, 1964.

[34] E. Z. Basta and M. A. Takla, "Mineralogy and Origin of Abu Ghalaga Ilmenite Occurrence, Eastern Desert," *Journal of Geology*, vol. 12, no. 2, pp. 87–124, 1968.

[35] M. E. Hilmy, M. L. Kabesh, G. S. Saleeb-Roufaiel, and A. M. Bishady, "Investigations on some mineral deposits in Um Rus area, Eastern Desert," *Journal of Geology*, *United Arab Republic*, vol. 12, no. 2, pp. 127-134, 1968.

[36] E. Z. Basta, "New Data on the System Fe2O3- FeTiO3-TiO2 (Ferri-Ilmenite and Titanom-agetite," *Proceeding Egyptian Academic Science*, vol. 14, pp. 1–15, 1959.

[37] E. F. Stumpfl, "Contribution to the study of ore minerals in some igneous rocks from Assynt," *Mineralogical magazine and journal of the Mineralogical Society*, vol. 32, no. 253, pp. 767–777, Jun. 1961, https://doi.org/10.1180/minmag.1961.032.253.03.

[38] A. B. Edwards, *Textures of the ore minerals and their significance.* Melbourne, VIC, Australia: Australasian Institute of Mining and Metallurgy, 1947.

[39] P. Ramdohr, *The Ore Minerals and Their Intergrowths*. Oxford, England: Pergamon Press, 1980.

[40] N. K. Rao and G. V. U. Rao, "Intergrowths in ilmenite of the beach sands of Kerala," *Mineralogical magazine and journal of the Mineralogical Society*, vol. 35, no. 269, pp. 118–130, Mar. 1965, https://doi.org/10.1180/minmag.1965.035.269.14.

[41] N. S. Hammoud, "Electrical separation in upgrading Egyptian beach zircon and rutile concentrates," in *XIIth International Mineral Processing Congress*, Sao Paolo, Brazil, 1977, pp. 100–124.

[42] E. M. Kara, M. Meghachou, and N. Aboubekr, "Contribution of Particles Size Ranges to Sand Friction," *Engineering, Technology & Applied Science Research*, vol. 3, no. 4, pp. 497–501, Aug. 2013, https://doi.org/10.48084/etasr.361.